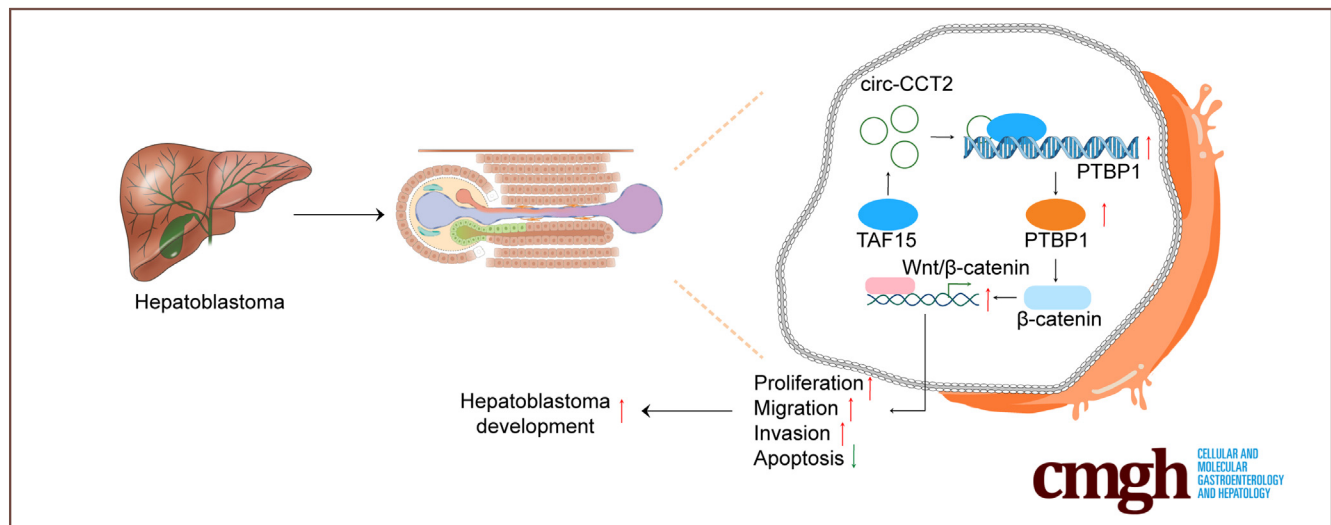# ORIGINAL RESEARCH

Circ-CCT2 Activates Wnt/β-catenin Signaling to Facilitate Hepatoblastoma Development by Stabilizing PTBP1 mRNA

Qin Zhu, Yu Hu, Wei Jiang, Zheng-Lin Ou, Yuan-Bing Yao, and Hong-Yan Zai

Department of General Surgery, Xiangya Hospital, Central South University, Changsha, Hunan Province, P.R. China

SUMMARY

Circ-CCT2, TAF15, and PTBP1 were up-regulated in hepatoblastoma, and circ-CCT2 activated the Wnt/β-catenin signaling and promoted the proliferation, migration, invasion, and EMT of hepatoblastoma cells via promoting TAF15 expression to stabilize PTBP1 mRNA in hepatoblastoma.

BACKGROUND & AIMS: Circ-CCT2 (hsa_circ_0000418) is a novel circular RNA that stems from the CCT2 gene. However, the expression of circ-CCT2 and its roles in hepatoblastoma are unknown. Our study aims to study the circ-CCT2 roles in hepatoblastoma development.

METHODS: Hepatoblastoma specimens were collected for examining the expression of circ-CCT2, TAF15, and PTBP1. CCK-8 and colony formation assays were applied for cell proliferation analysis. Migratory and invasive capacities were evaluated through wound healing and Transwell assays. The interaction between circ-CCT2, TAF15, and PTBP1 was validated by fluorescence in situ hybridization, RNA pull-down, and RNA immunoprecipitation. SKL2001 was used as an agonist of the Wnt/β-catenin pathway. A subcutaneous mouse model of

hepatoblastoma was established for examining the function of circ-CCT2 in hepatoblastoma in vivo.

RESULTS: Circ-CCT2 was significantly up-regulated in hepatoblastoma. Overexpression of circ-CCT2 activated Wnt/β-catenin signaling and promoted hepatoblastoma progression, whereas knockdown of circ-CCT2 exerted opposite effects. Moreover, both TAF15 and PTBP1 were up-regulated in hepatoblastoma tissues and cells. TAF15 was positively correlated with the expression of circ-CCT2 and PTBP1 in hepatoblastoma. Furthermore, circ-CCT2 recruited and up-regulated TAF15 protein to stabilize PTBP1 mRNA and trigger Wnt/β-catenin signaling in hepatoblastoma. Overexpression of TAF15 or PTBP1 reversed knockdown of circ-CCT2–mediated suppression of hepatoblastoma progression. SKL2001-mediated activation of Wnt/β-catenin signaling reversed the anti-tumor effects of silencing of circ-CCT2, TAF15, or PTBP1.

CONCLUSIONS: Circ-CCT2 stabilizes PTBP1 mRNA and activates Wnt/β-catenin signaling through recruiting and up-regulating TAF15 protein, thus promoting hepatoblastoma progression. Our findings deepen the understanding of hepatoblastoma pathogenesis and suggest potential therapeutic targets. *(Cell Mol Gastroenterol Hepatol 2024;17:175–197; https://doi.org/10.1016/j.jcmgh.2023.10.004)*

Hepatoblastoma is a rare type of liver cancer that primarily starts in the right lobe of the liver, but it is a common liver cancer in early childhood, affecting children younger than approximately 5 years of age.[1,2] Although the incidence is as low as 0.5–1.5 cases per 1,000,000 children, it is gradually increasing.[3,4] Multimodal therapy including surgery, chemotherapy, and liver transplantation are becoming standard treatment for hepatoblastoma.[5] Because of the advances of multimodal therapy and international cooperation, the prognosis of hepatoblastoma has been significantly improved. Systemic chemotherapy and surgery produce a good 5-year survival rate of more than 70% in children.[6] However, the prognosis is still poor for patients with unresectable hepatoblastoma.[3] Therefore, elucidating the pathogenesis of hepatoblastoma is vital for identifying novel biomarkers and therapeutic targets.

Circular RNAs (circRNAs) exert crucial biological activities in cancers.[7] Many circRNAs are implicated in regulating hepatoblastoma progression, such as circ-HMGCS1,[8] circ-CDR1as,[9] and circ-STAT3.[10] Chaperonin containing TCP1 subunit 2 (CCT2), a subunit of type II chaperonin composed of 2 stacked rings, is up-regulated in various cancers including lung, breast, prostate, and liver cancers and required for tumor growth.[11,12] Hsa_circ_0000418, also known as circ-CCT2, is a novel circular RNA that stems from the CCT2 gene. It has been reported that circ-CCT2 promotes glioma progression through miR-409-3p/PDK1 axis.[13] However, the roles of circ-CCT2 in hepatoblastoma are unknown.

TATA-box binding protein associated factor 15 (TAF15) plays key roles in RNA processing.[14] Bertolotti et al[15] first identified TAF15 as a component of transcription factor IID. Moreover, TAF15 interacts with RNA polymerase II and components of the spliceosome implicated in transcription and RNA splicing.[16] Intriguingly, TAF15 contains a RNA recognition motif and binds to the 3' untranslated region of target mRNAs to stabilize mRNAs.[17] TAF15 is highly abundant in cancers and acts as an oncogene. Ren et al[18] reported that TAF15 was recruited by PITPNA-AS1 to stabilize HMGB3 mRNA and promote lung squamous cell carcinoma progression. Because circRNAs can function as protein sponges, recruiters, and scaffolds,[19] we predicted that circ-CCT2 might bind to TAF15 through bioinformatics, suggesting the possibility that circ-CCT2 exerts functions by regulating TAF15 protein to regulate target mRNA stability. The interaction between circ-CCT2 and TAF15 and their roles has not been reported.

Polypyrimidine tract binding protein 1 (PTBP1) is highly expressed in many cancers and exerts oncogenic activity. PTBP1 is abundant in breast cancer, and it accelerates tumor growth by regulating PTEN/AKT pathway.[20] MAFG-AS1 promotes the progression of bladder urothelial carcinoma through HuR/PTBP1 axis.[21] Moreover, PTBP1 is up-regulated in hepatocellular carcinoma (HCC) and promotes HCC progression.[22] The expression of PTBP1 is modulated by dysregulated miRNAs during carcinogenesis to promote the progression of various cancers such as brain tumors, sarcomas, gastrointestinal cancers, and HCC.[23] Intriguingly, PTBP1 is recruited by lncRNA OIP5-AS1 to stabilize CTNNB1 mRNA and aggravate hepatoblastoma stemness.[24] We predicted that PTBP1 mRNA might be a target mRNA of TAF15 by bioinformatics, indicating that TAF15 might stabilize PTBP1 mRNA in hepatoblastoma. In addition, recent studies have found that PTBP1 is implicated in Wnt/β-catenin signaling.[25,26] Therefore, we hypothesized that PTBP1 might be regulated by TAF15 and implicated in hepatoblastoma through Wnt/β-catenin signaling.

Here we reported that circ-CCT2, TAF15, and PTBP1 were up-regulated in hepatoblastoma, which indicated the involvement of these 3 molecules in hepatoblastoma development. Indeed, we demonstrated that circ-CCT2 activated Wnt/β-catenin signaling and promoted hepatoblastoma progression via recruiting and up-regulating TAF15 protein to stabilize PTBP1 mRNA for the first time. Collectively, our study sheds novel light on the pathogenesis of hepatoblastoma and provides promising therapeutic targets.

Results

Circ-CCT2 Was Highly Expressed in Hepatoblastoma and Primarily Localized in the Cytoplasm

We analyzed the expression of circ-CCT2 in hepatoblastoma and adjacent normal tissues from hepatoblastoma patients. Compared with normal tissues, hepatoblastoma tissues showed the increased expression of circ-CCT2 (Figure 1*A*). Elevated expression of circ-CCT2 was also observed in human hepatoblastoma cells including HuH-6 and HepG2 cells (Figure 1*B*). Fluorescence in situ hybridization (FISH) assay showed predominant cytoplastic localization of circ-CCT2 in HuH-6 and HepG2 cells (Figure 1*C*). Furthermore, nuclear and cytoplastic fractions were separated, and we found that circ-CCT2 was mainly enriched in the cytoplasm (Figure 1*D*). Because circRNAs are generated through back-splicing,[27] the back-splicing junction of circ-CCT2 was validated by Sanger sequencing (Figure 1*E*). Compared with linear RNAs such as mRNAs, circRNAs are highly stable thanks to the circular structure,[28] which is commonly analyzed by RNase R digestion and actinomycin D treatment.[29,30] As shown in Figure 1*F*, total RNA isolated from HuH-6 and HepG2 cells were treated with RNase R, and circ-CCT2 was resistant to RNase R digestion compared with CCT2 mRNA. In addition, after actinomycin D treatment, circ-CCT2
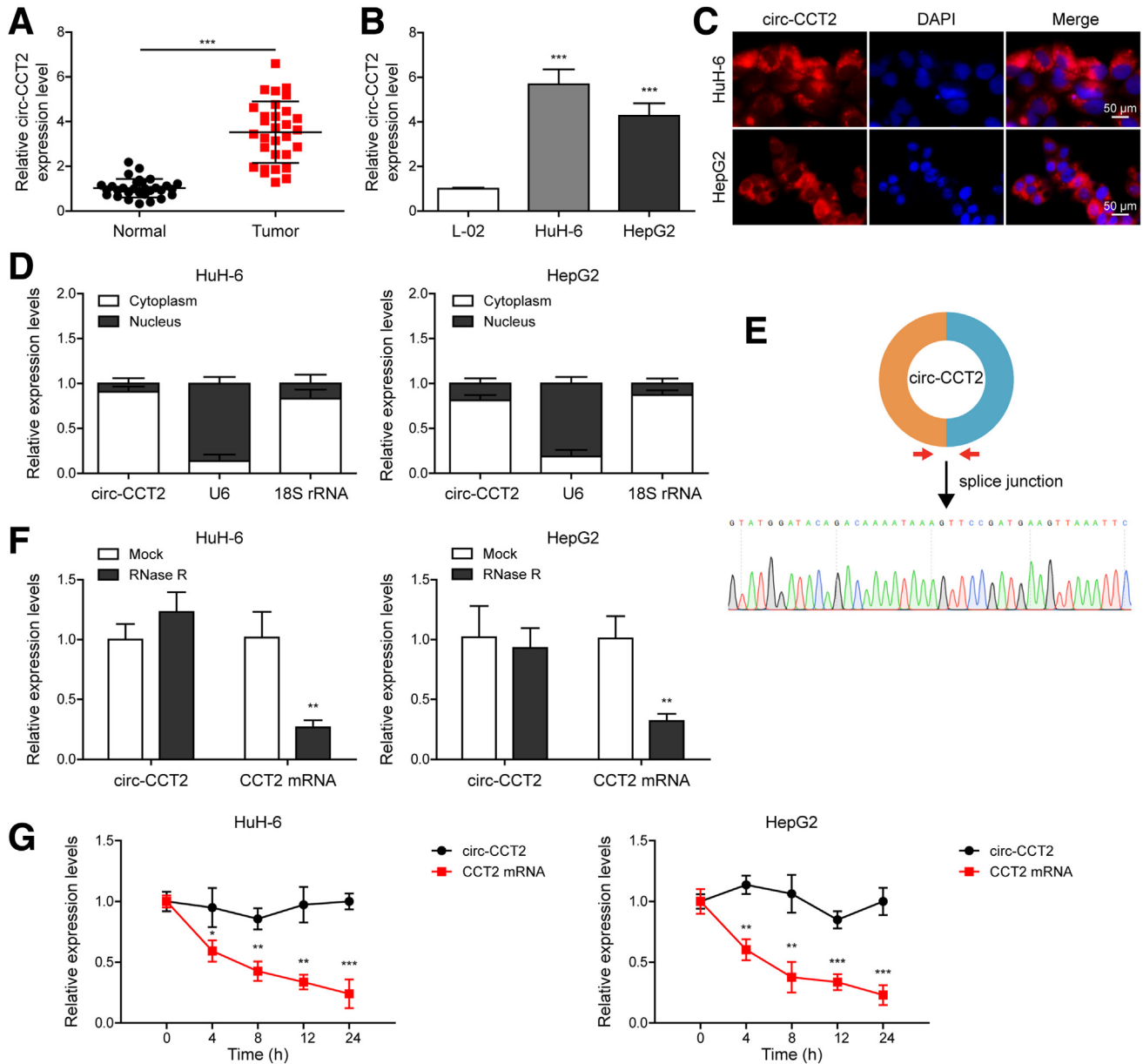
Most current article

Figure 1. Circ-CCT2 was highly expressed in hepatoblastoma tissues and cells and primarily localized in the cytoplasm. (*A*) qRT-PCR analysis of circ-CCT2 expression in hepatoblastoma and adjacent normal tissues (n = 30). (*B*) qRT-PCR analysis of circ-CCT2 expression in L-02, HuH-6, and HepG2 cells. (*C*) Localization of circ-CCT2 (*red*) was examined using FISH assay. Nuclei were stained with DAPI (*blue*). Scale bar = 50 μm. (*D*) Abundance of circ-CCT2 in cytoplastic and nuclear fractions separated from HuH-6 and HepG2 cells. U6 and 18S rRNA was used as nuclear and cytoplastic references, respectively. (*E*) Sanger sequencing was applied to validate the head-to-tail spliced structure of circ-CCT2. (*F*) Abundance of circ-CCT2 and CCT2 mRNA in response to RNase R digestion. (*G*) Stability of circ-CCT2 and CCT2 mRNA in HuH-6 and HepG2 cells after actinomycin D treatment was examined using qRT-PCR. *$P < .05$, **$P < .01$, ***$P < .001$.

was highly stable with a half-life of more than 24 hours, whereas CCT2 mRNA only had a half-life of about 4 hours (Figure 1*G*). These observations confirmed classical circular structure and stability of circ-CCT2.

Circ-CCT2 Promoted Malignant Phenotypes of Hepatoblastoma and Activated Wnt/B-catenin Signaling

To investigate the roles of circ-CCT2 in hepatoblastoma, HuH-6 and HepG2 cells were transfected with the circ-CCT2-overexpressing vector (OE-circ-CCT2) or short hairpin RNA (shRNA) against circ-CCT2 (sh-circ-CCT2) for its overexpression or knockdown. We confirmed that circ-CCT2 (Figure 2*A*), not linear CCT2 mRNA (Figure 2*B*), was efficiently overexpressed or knocked down in HuH-6 and HepG2 cells by quantitative real-time polymerase chain reaction (qRT-PCR). Overexpression of circ-CCT2 promoted the proliferation and colony formation of HuH-6 and HepG2 cells, whereas knockdown of circ-CCT2 suppressed cell proliferation and colony formation (Figure 2*C* and *D*).
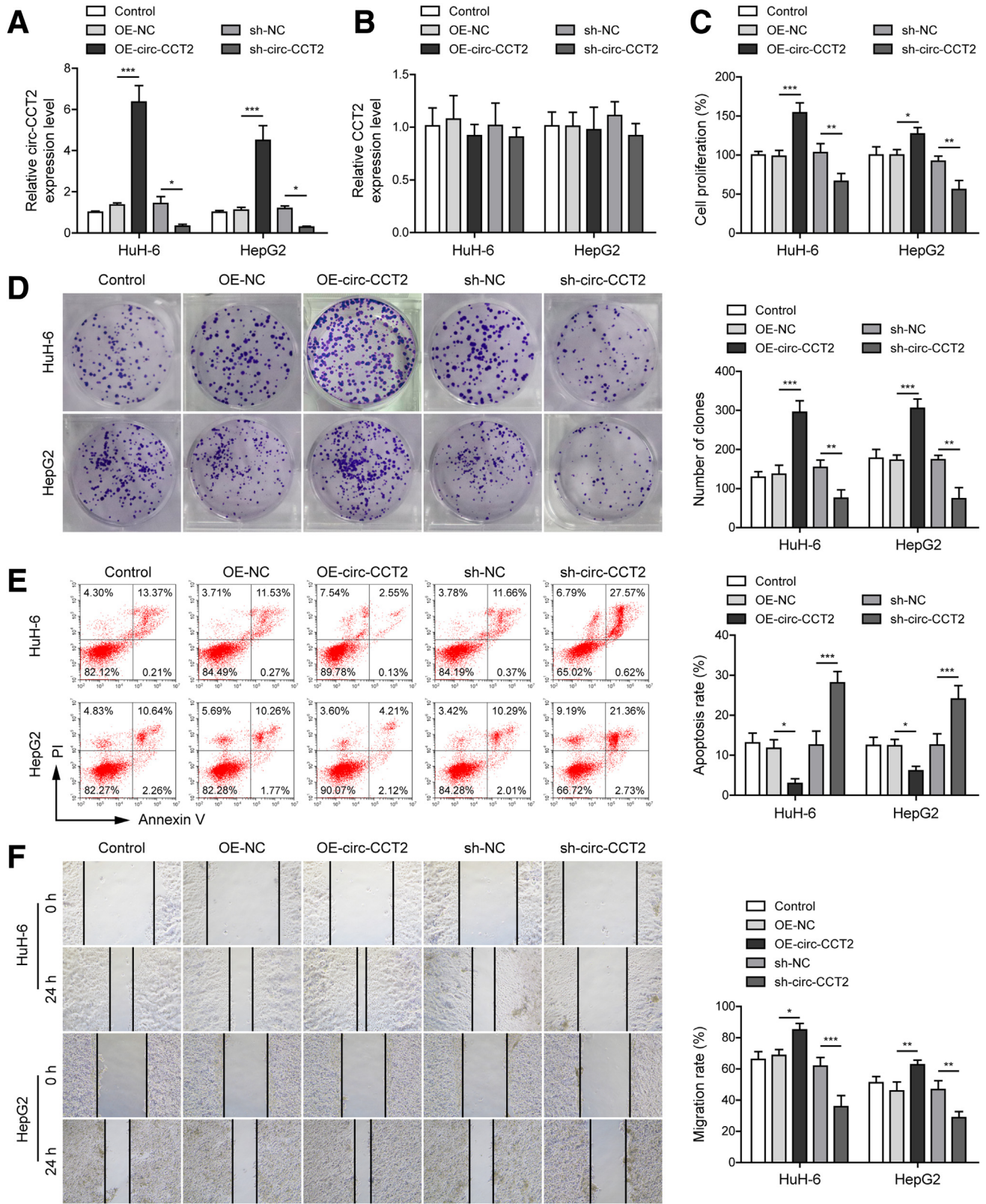
Figure 2. Circ-CCT2 promoted the proliferation and migration of hepatoblastoma cells. HuH-6 and HepG2 cells were transfected with OE-NC, OE-circ-CCT2, sh-NC, or sh-circ-CCT2 vector. Untransfected cells were used as control. (*A* and *B*) Expression levels of circ-CCT2 and linear CCT2 mRNA were assessed by qRT-PCR. (*C* and *D*) Cell proliferation was evaluated by CCK-8 and colony formation assays. (*E*) HuH-6 and HepG2 cell apoptosis was examined by Annexin V and PI staining. (*F*) Migratory capacities of HuH-6 and HepG2 cells were evaluated by wound healing assay. *$P < .05$, **$P < .01$, ***$P < .001$.

Besides, circ-CCT2-overexpressing cells showed reduced apoptosis, but increased apoptosis was observed in cells with knockdown of circ-CCT2 (Figure 2E). Subsequently, we examined cell migration and invasion by wound healing (Figure 2F) and Transwell (Figure 3A) assays, respectively. The migratory and invasive capacities of HuH-6 and HepG2 cells were suppressed by knockdown of circ-CCT2, but overexpression of circ-CCT2 significantly promoted hepatoblastoma cell migration and invasion (Figure 2F, Figure 3A). Furthermore, we found that levels of Slug, MMP-9, and N-cadherin were significantly increased, and E-cadherin was down-regulated by overexpression of circ-CCT2 in HuH-6 and HepG2 cells, but knockdown of circ-CCT2 exerted opposite effects on the expression of these endothelial-mesenchymal transition (EMT)-related factors (Figure 3B), suggesting that circ-CCT2 promoted EMT in hepatoblastoma. The expression of β-catenin and downstream targets of Wnt/β-catenin signaling such as c-Myc, Cyclin D1, and LGR5 were enhanced in circ-CCT2-overexpressing HuH-6 and HepG2 cells but inhibited by knockdown of circ-CCT2 (Figure 3B). Another downstream target of Wnt/β-catenin signaling, DKK1, was reduced after overexpression of circ-CCT2, whereas knockdown of circ-CCT2 promoted DKK1 expression (Figure 3B), indicating that circ-CCT2 activated Wnt/β-catenin signaling in hepatoblastoma cells. Collectively, our findings indicated that circ-CCT2 promoted the progression of hepatoblastoma through activation of Wnt/β-catenin signaling in hepatoblastoma cells.

Circ-CCT2 Accelerated Hepatoblastoma Growth and EMT and Activated Wnt/B-catenin Signaling in Vivo

HuH-6 and HepG2 cells were stably transfected with OE-circ-CCT2 or sh-circ-CCT2 vector through lentiviral transduction and subcutaneously injected into mice. The volume and weight of tumors formed by circ-CCT2-overexpressing cells were significantly increased (Figure 4A–C). However, silencing of circ-CCT2 reduced tumor volume and weight (Figure 4A–C). Immunohistochemical staining assay showed that the expression of Ki-67 (Figure 4D) and N-cadherin (Figure 4E) were promoted by overexpression of circ-CCT2 but suppressed by knockdown of circ-CCT2. Moreover, we confirmed that circ-CCT2 was overexpressed or knocked down in tumors by qRT-PCR through transfection of OE-circ-CCT2 or sh-circ-CCT2 vector (Figure 4F). In addition, the expression levels of β-catenin, c-Myc, Cyclin D1, and LGR5 were up-regulated in tumors formed by circ-CCT2-overexpressing cells and down-regulated in tumors formed by circ-CCT2-silencing cells (Figure 4G). DKK1 was down-regulated in tumors formed by circ-CCT2-overexpressing cells but was up-regulated in tumors formed by circ-CCT2-silencing cells (Figure 4G). These results demonstrated that circ-CCT2 enhanced the growth and EMT of hepatoblastoma and activated Wnt/β-catenin signaling in vivo.

Circ-CCT2 Bound to TAF15 and Positively Regulated Its Protein Expression in Hepatoblastoma

Because circRNAs can bind to RNA-binding proteins,[31] we used RNA immunoprecipitation (RIP) assay to show that circ-

CCT2 was significantly enriched in the anti-TAF15–immunoprecipitated fraction in HuH-6 and HepG2 cells (Figure 5A). Moreover, TAF15 could be efficiently pulled down by the biotin-conjugated sense circ-CCT2, but not by the anti-sense circ-CCT2 probe (Figure 5B). Then, we examined the co-localization of circ-CCT2 and TAF15 protein in hepatoblastoma cells (Figure 5C) and tissues (Figure 5D) by FISH and immunofluorescence (IF) staining. More cytoplastic co-localization of circ-CCT2 and TAF15 protein was observed. These data suggested that circ-CCT2 might directly interact with TAF15 in the cytoplasm. We also validated that TAF15 was highly expressed in hepatoblastoma tissues (Figure 5E and F) and cells (Figure 5G and H) compared with normal tissues and L-02 and minor histocompatibility antigen (MIHA) cells by qRT-PCR and Western blotting. The protein expression of TAF15 was enhanced by overexpression of circ-CCT2 and inhibited by knockdown of circ-CCT2 in HuH-6 and HepG2 cells (Figure 5I). Also, the expression of TAF15 was positively correlated with circ-CCT2 expression in hepatoblastoma tissues (Figure 5J), suggesting that circ-CCT2 recruited and up-regulated TAF15 protein in hepatoblastoma.

Overexpression of TAF15 Abrogated Knockdown of Circ-CCT2–Mediated Suppression of Malignant Phenotypes and Wnt/B-catenin Signaling in Hepatoblastoma

To investigate whether circ-CCT2–mediated regulation in hepatoblastoma is dependent on TAF15, HuH-6 and HepG2 cells were transfected with sh-circ-CCT2 or sh-circ-CCT2 in combination with the TAF15-overexpressing vector (pcDNA3.1-TAF15). Compared with controls, the expression of TAF15 was decreased in cells transfected with sh-circ-CCT2, whereas it was dramatically enhanced by simultaneous transfection of pcDNA3.1-TAF15 (Figure 6A). Knockdown of circ-CCT2–mediated suppressive effects on hepatoblastoma cell proliferation and colony formation was largely reversed by overexpression of TAF15 (Figure 6B and C). Increased apoptosis of HuH-6 and HepG2 cells transfected with sh-circ-CCT2 was suppressed by overexpression of TAF15 (Figure 6D). Furthermore, knockdown of circ-CCT2 weakened migratory (Figure 6E) and invasive (Figure 7A) capacities of HuH-6 and HepG2 cells, which were largely reversed by overexpression of TAF15. The expression of Slug and MMP-9 and E- to N-cadherin switch were suppressed in cells transfected with sh-circ-CCT2, but simultaneous overexpression of TAF15 reversed these effects (Figure 7B). Moreover, overexpression of TAF15 abolished knockdown of circ-CCT2–mediated suppression of the expression of β-catenin, c-Myc, and Cyclin D1 in HuH-6 and HepG2 cells (Figure 7B). These results suggested that circ-CCT2 silencing-mediated suppression of malignant phenotypes and Wnt/β-catenin signaling was dependent on targeting TAF15 in hepatoblastoma cells.

PTBP1 Was Highly Expresssed and Acted as a Target of TAF15 in Hepatoblastoma

Because TAF15 is an RNA binding protein and regulates the stability of target mRNAs,[17,18] we predicted PTBP1
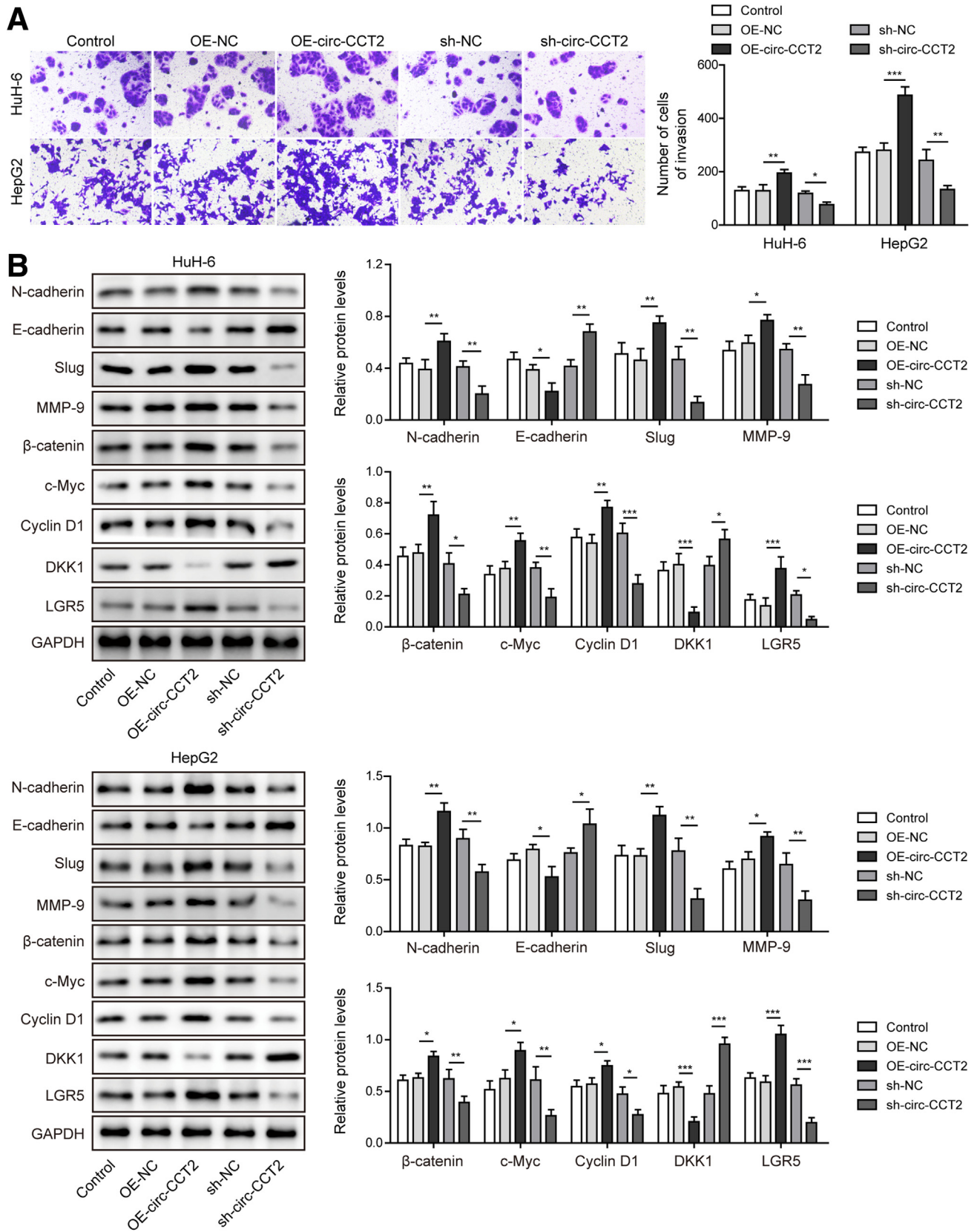
Figure 3. Circ-CCT2 promoted invasion and EMT of hepatoblastoma cells and activated Wnt/β-catenin signaling. HuH-6 and HepG2 cells were transfected with OE-NC, OE-circ-CCT2, sh-NC, or sh-circ-CCT2 vector. Untransfected cells were used as control. (*A*) Invasive capacities of HuH-6 and HepG2 cells were evaluated by Transwell assay. (*B*) Protein levels of N-cadherin, E-cadherin, Slug, MMP-9, β-catenin, c-Myc, Cyclin D1, DKK1, and LGR5 in HuH-6 and HepG2 cells were analyzed by Western blotting and normalized to GAPDH. *P < .05, **P < .01, ***P < .001.
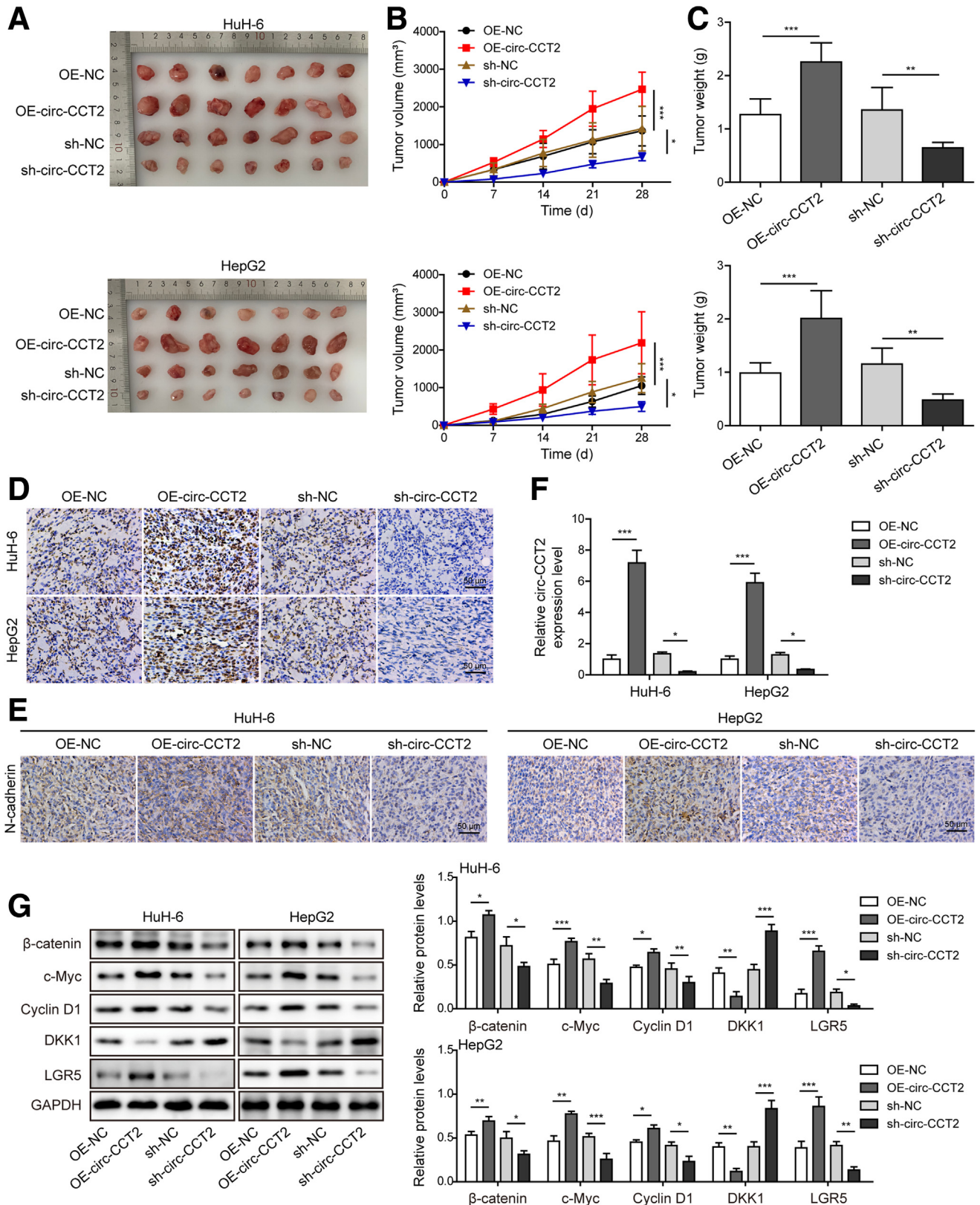
Figure 4. Circ-CCT2 accelerated hepatoblastoma growth and EMT and activated Wnt/β-catenin signaling in vivo. HuH-6 and HepG2 cells were stably transfected with OE-NC, OE-circ-CCT2, sh-NC, or sh-circ-CCT2 through lentiviral transduction and subcutaneously injected into the left flanks of mice (n = 7 in each group). (A) Images of excised tumors. (B) Tumor volume. (C) Tumor weight. (D and E) Immunohistochemical staining of Ki-67 and N-cadherin expression in tumors. Scale bar = 50 μm. (F) qRT-PCR analysis of circ-CCT2 in tumors. (G) Protein levels of β-catenin, c-Myc, Cyclin D1, DKK1, and LGR5 in tumors were analyzed by Western blotting and normalized to GAPDH. *P < .05, **P < .01, ***P < .001.
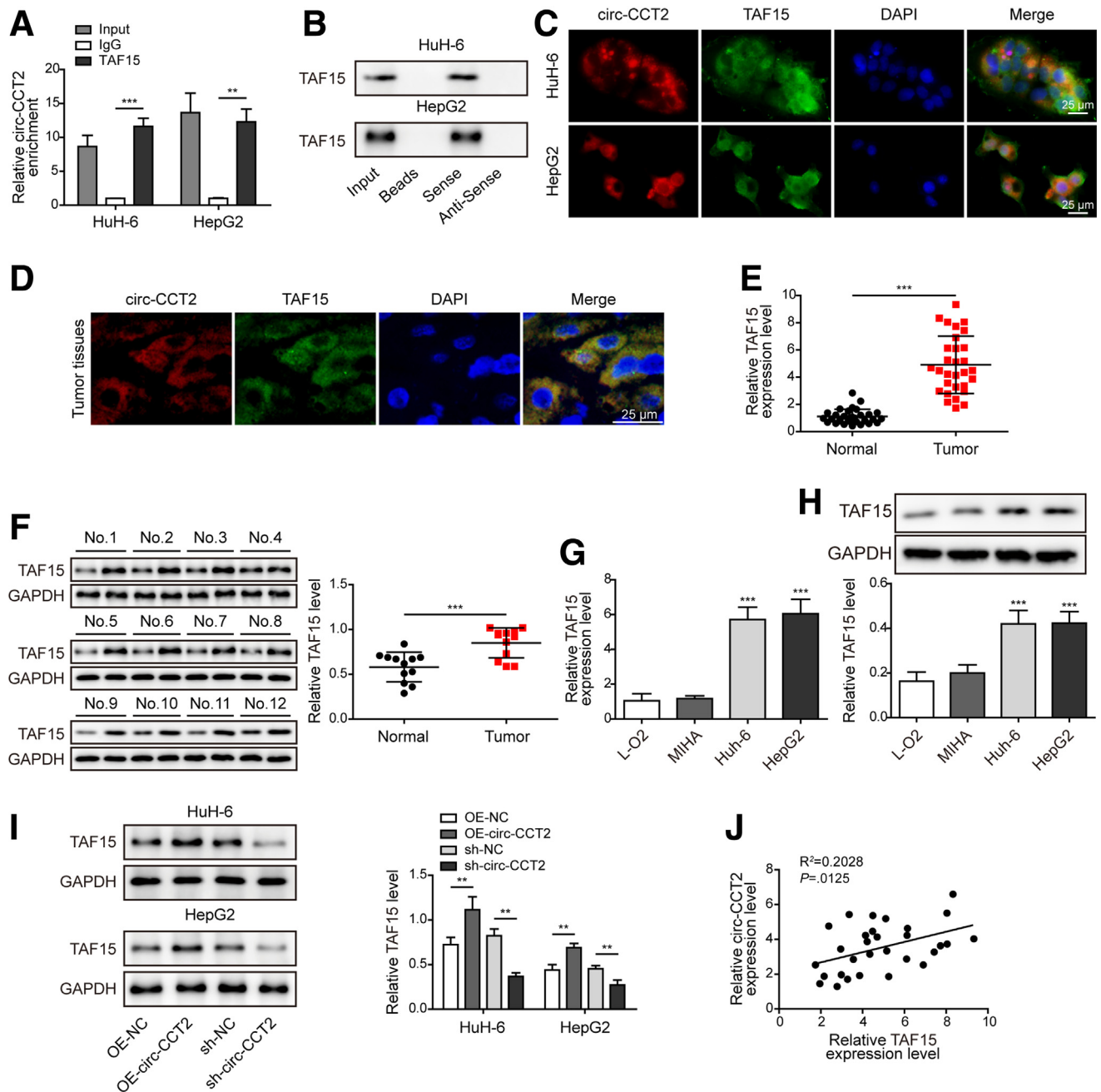
Figure 5. Circ-CCT2 recruited TAF15 and positively regulated its protein expression in hepatoblastoma. (*A*) Enrichment of circ-CCT2 was examined in anti-TAF15–immunoprecipitated fractions from HuH-6 and HepG2 cells. Normal immuno-globulin G was used as negative control. (*B*) Abundance of TAF15 in input and fractions pulled down by beads (without probes); the biotin-conjugated sense or anti-sense circ-CCT2 probes were detected by Western blotting. (*C* and *D*) Locali-zation of circ-CCT2 (*red*) and TAF15 (*green*) in HuH-6 and HepG2 cells and tumor and adjacent normal tissues were examined by FISH and IF staining. Nuclei were stained with DAPI (*blue*). Scale bar = 25 μm. (*E*) qRT-PCR analysis of TAF15 expression in hepatoblastoma and adjacent normal tissues (n = 30). (*F*) Protein levels of TAF15 were examined in hepatoblastoma and adjacent normal tissues (n = 12). (*G* and *H*) Expression of TAF15 in L-02, MIHA, HuH-6, and HepG2 cells was assessed by qRT-PCR and Western blotting. (*I*) Western blotting analysis of TAF15 expression in HuH-6 and HepG2 cells transfected with OE-NC, OE-circ-CCT2, sh-NC, or sh-circ-CCT2 vector. GAPDH was used as normalization control. (*J*) Correlation analysis of expression of circ-CCT2 and TAF15 in hepatoblastoma tissues (n = 30). **$P < .01$, ***$P < .001$.

mRNA as a target mRNA of TAF15 (Figure 8*A*). Compared with normal tissues, hepatoblastoma tissues showed increased expression of PTBP1 (Figure 8*B*). Moreover, elevated PTBP1 expression was also observed in HuH-6 and

HepG2 cells compared with L-02 and MIHA cells (Figure 8*C* and *D*). Subsequently, we found that PTBP1 was efficiently enriched in the anti-TAF15-immunoprecipitated fractions from HuH-6 and HepG2 cells (Figure 8*E*). FISH combined IF
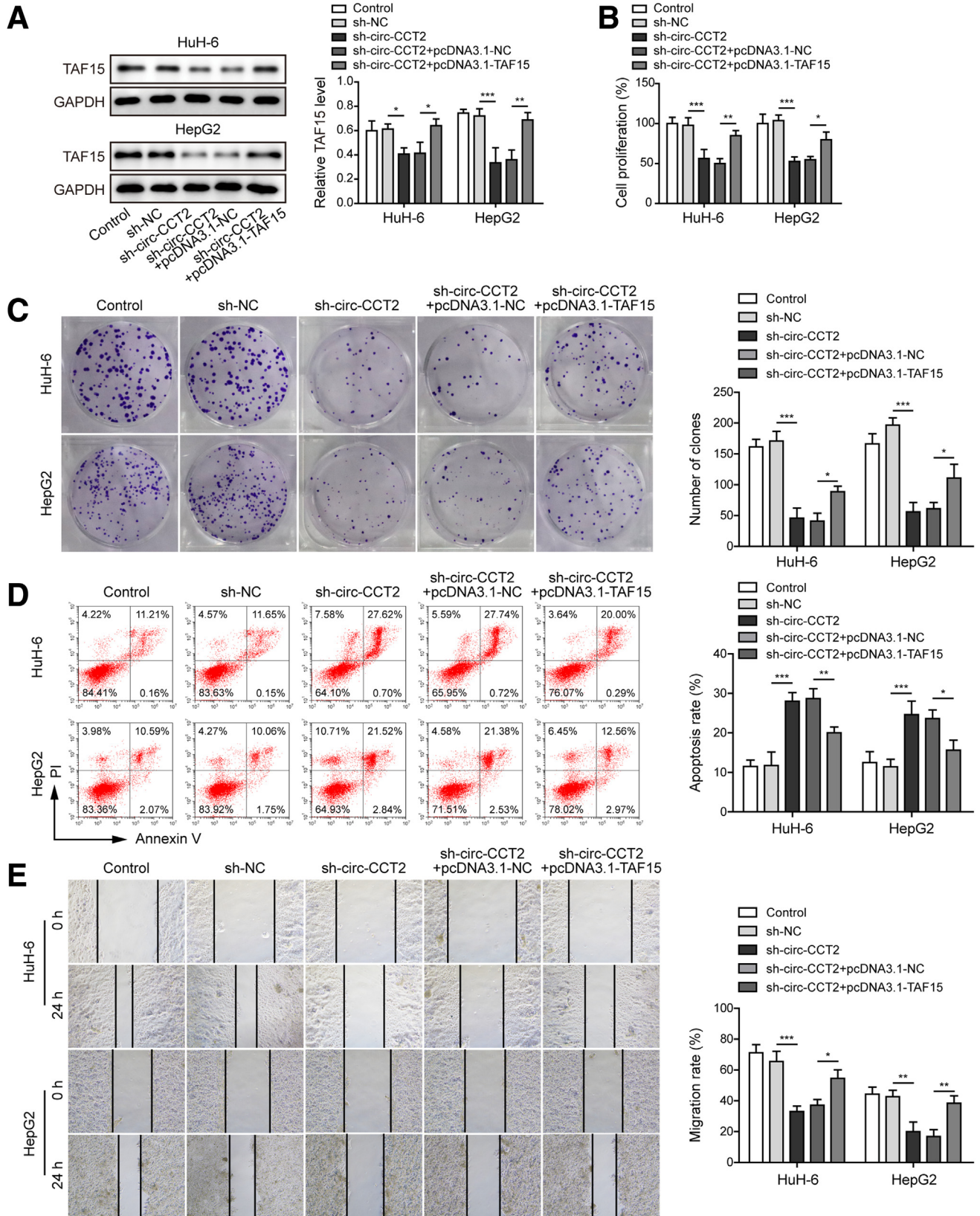
Figure 6. Overexpression of TAF15 abrogated knockdown of circ-CCT2–mediated suppression on proliferation and migration in hepatoblastoma. HuH-6 and HepG2 cells were transfected with sh-NC, sh-circ-CCT2, sh-circ-CCT2+pcDNA3.1-NC, or sh-circ-CCT2+pcDNA3.1-TAF15. Untransfected cells were used as control. (*A*) Expression of TAF15 was analyzed by Western blotting. (*B* and *C*) Cell proliferation was evaluated by CCK-8 and colony formation assays. (*D*) Cell apoptosis was analyzed by Annexin V and PI staining. (*E*) Migratory capacities of HuH-6 and HepG2 cells were evaluated by wound healing assay. *$P < .05$, **$P < .01$, ***$P < .001$.
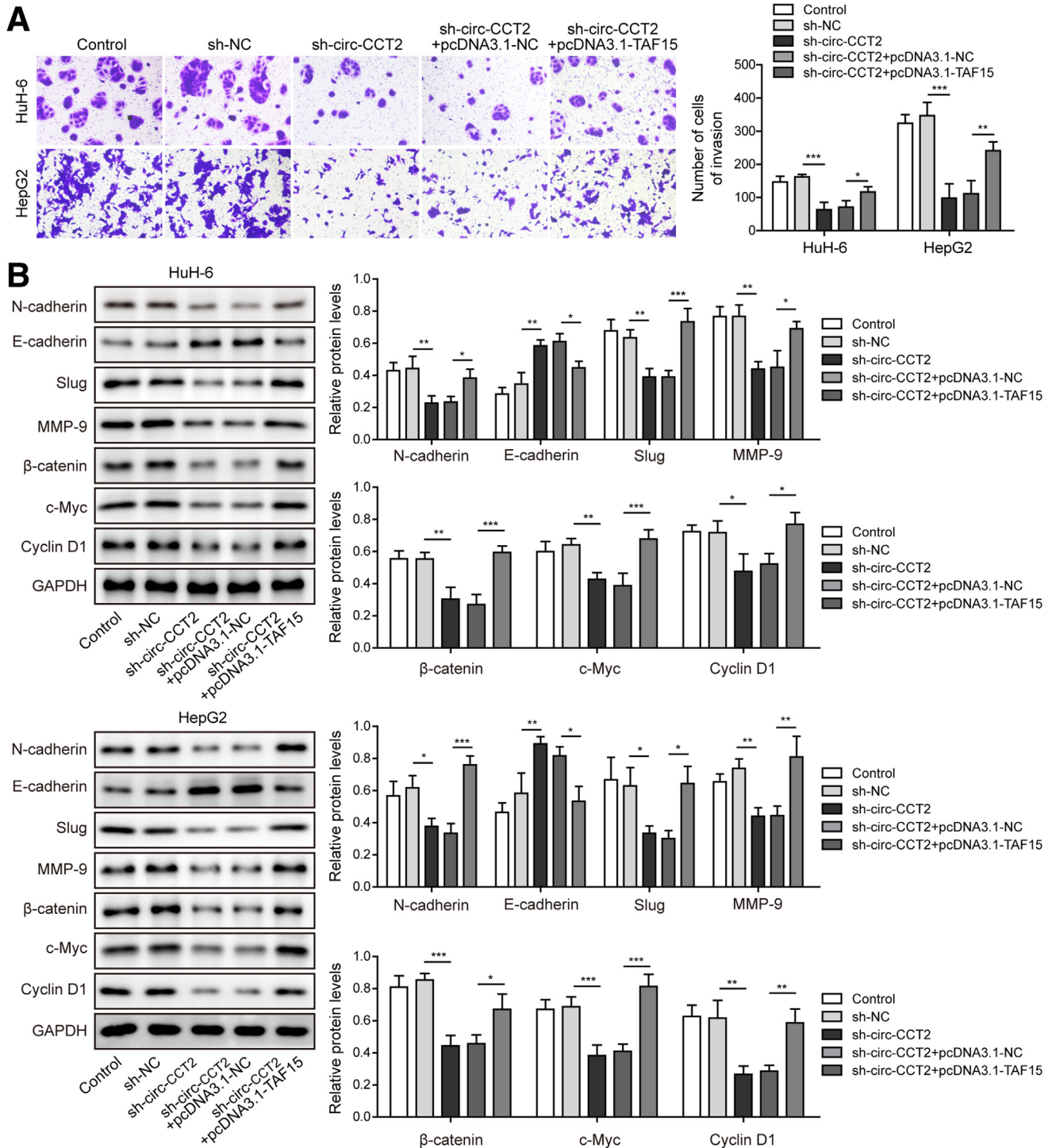
Figure 7. Overexpression of TAF15 abrogated knockdown of circ-CCT2–mediated suppression on invasion, EMT, and Wnt/β-catenin signaling in hepatoblastoma. HuH-6 and HepG2 cells were transfected with sh-NC, sh-circ-CCT2, sh-circ-CCT2+pcDNA3.1-NC, or sh-circ-CCT2+pcDNA3.1-TAF15. Untransfected cells were used as control. (*A*) Invasive capacities of HuH-6 and HepG2 cells were evaluated by Transwell assay. (*B*) Protein levels of N-cadherin, E-cadherin, Slug, MMP-9, β-catenin, c-Myc, and Cyclin D1 in HuH-6 and HepG2 cells were analyzed by Western blotting and normalized to GAPDH. *$P <$ .05, **$P <$ .01, ***$P <$ .001.

assays showed cytoplasmic co-localization of TAF15 protein and PTBP1 mRNA in HuH-6 and HepG2 cells (Figure 8*F*) and tumor tissues (Figure 8*G*). Overexpression of TAF15 promoted the mRNA and protein expression of PTBP1, whereas knockdown of TAF15 reduced its expression in HuH-6 and HepG2 cells (Figure 8*H–J*). Furthermore, the

stability of PTBP1 mRNA after actinomycin D treatment was increased by overexpression of TAF15 (Figure 8K). In addition, the expression of TAF15 and PTBP1 were positively correlated in hepatoblastoma tissues (Figure 8L). To conclude, our findings demonstrated that TAF15 directly bound to PTBP1 mRNA and promoted its stability in hepatoblastoma.

Overexpression of PTBP1 Reversed Knockdown of TAF15-Mediated Inhibition of Malignancy and Wnt/β-catenin Signaling in Hepatoblastoma

HuH-6 and HepG2 cells were transfected with sh-TAF15 or sh-TAF15 in combination with the PTBP1-overexpressing vector (pcDNA3.1-PTBP1). The expression of TAF15 and PTBP1 was reduced by transfection of sh-TAF15 in HuH-6 and HepG2 cells, and PTBP1 was markedly up-regulated by transfection of pcDNA3.1-PTBP1 (Figure 9A–C). Overexpression of PTBP1 did not affect the expression of TAF15 (Figure 9A–C). Knockdown of TAF15 repressed the proliferation and colony formation of HuH-6 and HepG2 cells, which were largely reversed by simultaneous overexpression of PTBP1 (Figure 9D and E). HuH-6 and HepG2 cell apoptosis was induced by knockdown of TAF15 but inhibited by overexpression of PTBP1 (Figure 9F). Besides, simultaneous overexpression of PTBP1 abolished knockdown of TAF15-mediated suppressive effects on cell migration and invasion (Figure 10A and B). The expression of EMT-related factors and E- to N-cadherin switch were inhibited in cells transfected with sh-TAF15, and the suppressive effects were reversed by simultaneous overexpression of PTBP1 (Figure 10C). In addition, knockdown of TAF15 reduced the expression of β-catenin, c-Myc, and Cyclin D1, and overexpression of PTBP1 restored their expression in HuH-6 and HepG2 cells (Figure 10C). These data implied that TAF15 regulated tumor progression and Wnt/β-catenin signaling by regulating PTBP1 in hepatoblastoma.

Overexpression of PTBP1 Reversed Knockdown of Circ-CCT2–Mediated Inhibition of Malignant Phenotypes and Wnt/B-catenin Signaling in Hepatoblastoma

HuH-6 and HepG2 cells were transfected with sh-circ-CCT2 or sh-circ-CCT2 in combination with pcDNA3.1-TAF15 and treated with actinomycin D for evaluating the stability of PTBP1 mRNA. Compared with sh-NC group, the stability of PTBP1 mRNA was obviously impaired in cells transfected with sh-circ-CCT2, but overexpression of TAF15 significantly improved its mRNA stability (Figure 11A). Subsequently, we found that the enrichment of PTBP1 in anti-TAF15-immunoprecipitated fractions was markedly reduced by knockdown of circ-CCT2 (Figure 11B). We then examined the expression of circ-CCT2, TAF15, and PTBP1 in HuH-6 and HepG2 cells transfected with sh-circ-CCT2 or sh-circ-CCT2 in combination with pcDNA3.1-PTBP1. Circ-CCT2, TAF15, and PTBP1 were down-regulated in cells transfected with sh-circ-CCT2 (Figure 11C–F). The expression levels of circ-CCT2 and TAF15 were unaffected, but PTBP1 was obviously up-regulated by transfection of pcDNA3.1-PTBP1 (Figure 11C–F). Knockdown of circ-CCT2–mediated suppression of cell proliferation (Figure 11G), colony formation (Figure 11H), migration (Figure 12A), and invasion (Figure 12B), and enhancement of cell apoptosis (Figure 11I) in HuH-6 and HepG2 cells were largely reversed by simultaneous overexpression of PTBP1. The suppressive expression of EMT and Wnt/β-catenin signaling-related factors in sh-circ-CCT2–transfected cells was abrogated by simultaneous overexpression of PTBP1 (Figure 12C). In addition, circ-CCT2 silencing-mediated up-regulation of DKK1 and down-regulation of LGR5 were reversed by PTBP1 overexpression (Figure 12C). These results demonstrated that circ-CCT2 promoted malignant phenotypes and Wnt/β-catenin signaling by stabilizing PTBP1 mRNA through up-regulating TAF15 in hepatoblastoma.

Activation of Wnt/B-catenin Signaling Reversed Knockdown of Circ-CCT2, TAF15, or PTBP1-Mediated Inhibition of Malignant Phenotypes of Hepatoblastoma

To validate Wnt/β-catenin as the downstream signaling for the circ-CCT2/TAF15/PTBP1 axis, we treated circ-CCT2, TAF15, or PTBP1-knockdown HuH-6 and HepG2 cells with SKL2001, an agonist of Wnt/β-catenin pathway. We found that down-regulation of β-catenin and LGR5 and up-regulation of DKK1 in circ-CCT2, TAF15, or PTBP1-knockdown cells were abrogated by SKL2001 treatment (Figure 13A). Furthermore, we verified the LGR5 and DKK1 expression levels in hepatoblastoma tissues, and results proved that DKK1 was decreased and LGR5 was increased in hepatoblastoma tissues compared with normal tissues (Figure 13B). Correlation analyses showed that DKK1 expression was negatively correlated with the expression of circ-CCT2, TAF15, and PTBP1 (Figure 13C), and LGR5 expression was positively correlated with the expression of circ-CCT2, TAF15, and PTBP1 in tumor tissues (Figure 13D). Then, knockdown of circ-CCT2, TAF15, or PTBP1 enhanced HuH-6 and HepG2 cell apoptosis (Figure 14A and B) and impaired cell invasion (Figure 14C and D) and proliferation (Figure 14E), but these anti-tumor effects were partly counteracted by SKL2001 treatment (Figure 14A–E). These data validated that the circ-CCT2/TAF15/PTBP1 axis promoted hepatoblastoma development through activating Wnt/β-catenin signaling.

Discussion

Hepatoblastoma is rare, but its incidence is increasing, and most patients who suffer from hepatoblastoma are children.[32] The overall survival for hepatoblastoma at all stages is relatively good, but the mortality is very high for advanced hepatoblastoma and adolescent and adult patients.[3,33,34] Clarifying the regulatory mechanism of hepatoblastoma progression is essential for developing novel therapies and improving prognosis for hepatoblastoma. In
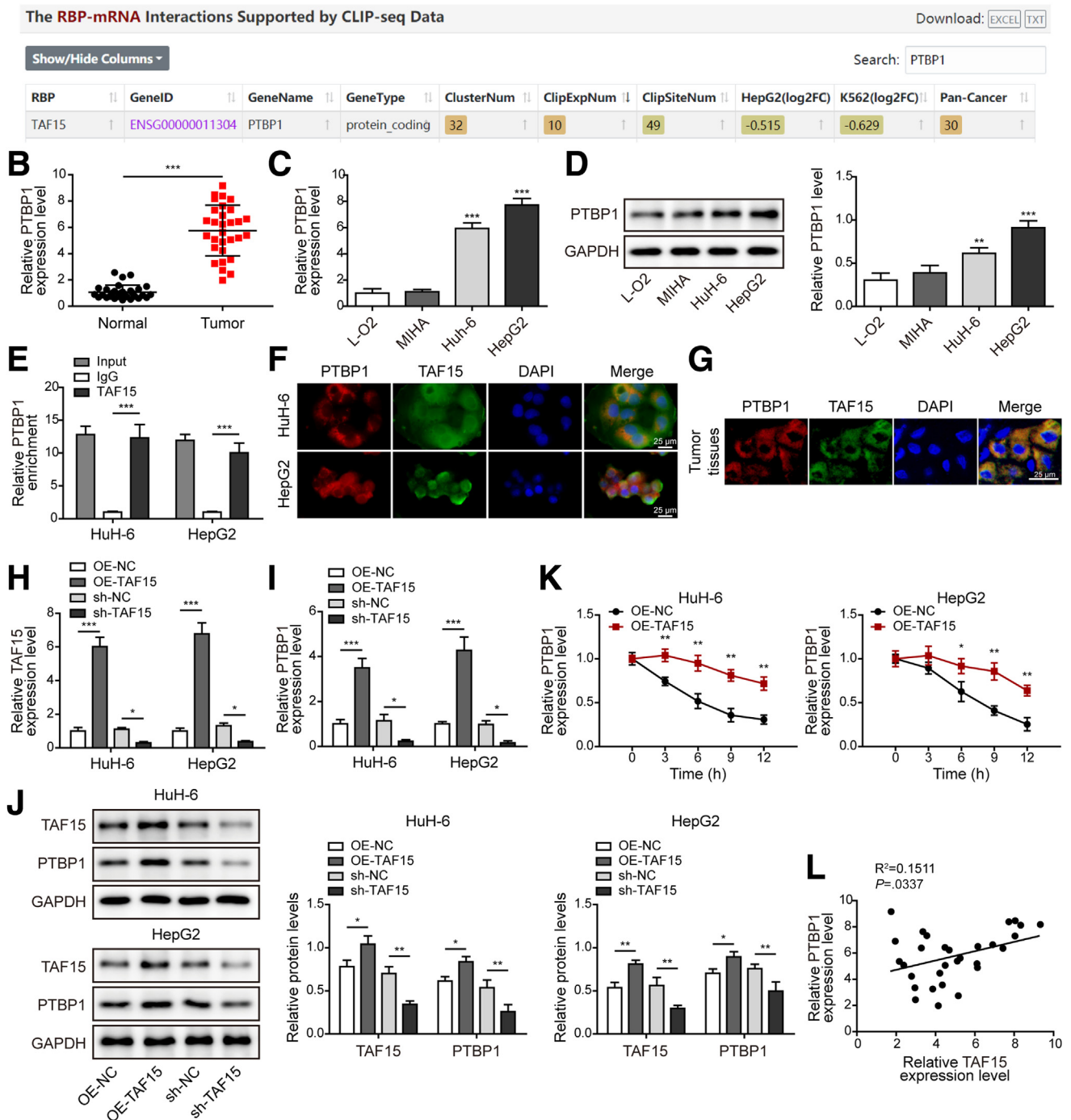
Figure 8. PTBP1 was highly expressed and acted as a target of TAF15 in hepatoblastoma. (*A*) PTBP1 mRNA was predicted to be a target mRNA of TAF15 by bioinformatics. (*B*) qRT-PCR analysis of PTBP1 expression in hepatoblastoma and adjacent normal tissues (n = 30). (*C* and *D*) Expression of PTBP1 in L-02, MIHA, HuH-6, and HepG2 cells was assessed by qRT-PCR and Western blotting. (*E*) Enrichment of PTBP1 mRNA was examined in input and anti-TAF15–immunoprecipitated fractions from HuH-6 and HepG2 cells. Normal immunoglobulin G was used as negative control. (*F* and *G*) Localization of PTBP1 mRNA (*red*) and TAF15 (*green*) in HuH-6 and HepG2 cells and tumor and adjacent normal tissues were examined by FISH and IF staining. Nuclei were stained with DAPI (*blue*). Scale bar = 25 μm. (*H* and *I*) qRT-PCR analyses of TAF15 and PTBP1 in HuH-6 and HepG2 cells transfected with pcDNA3.1-NC, pcDNA3.1-TAF15, sh-NC, or sh-TAF15. (*J*) Protein levels of TAF15 and PTBP1 were analyzed by Western blotting. (*K*) Stability of PTBP1 mRNA after actinomycin D treatment was examined using qRT-PCR. (*L*) Correlation analysis of expression of PTBP1 and TAF15 in hepatoblastoma tissues (n = 30). *$P <$ .05, **$P <$ .01, ***$P <$ .001.
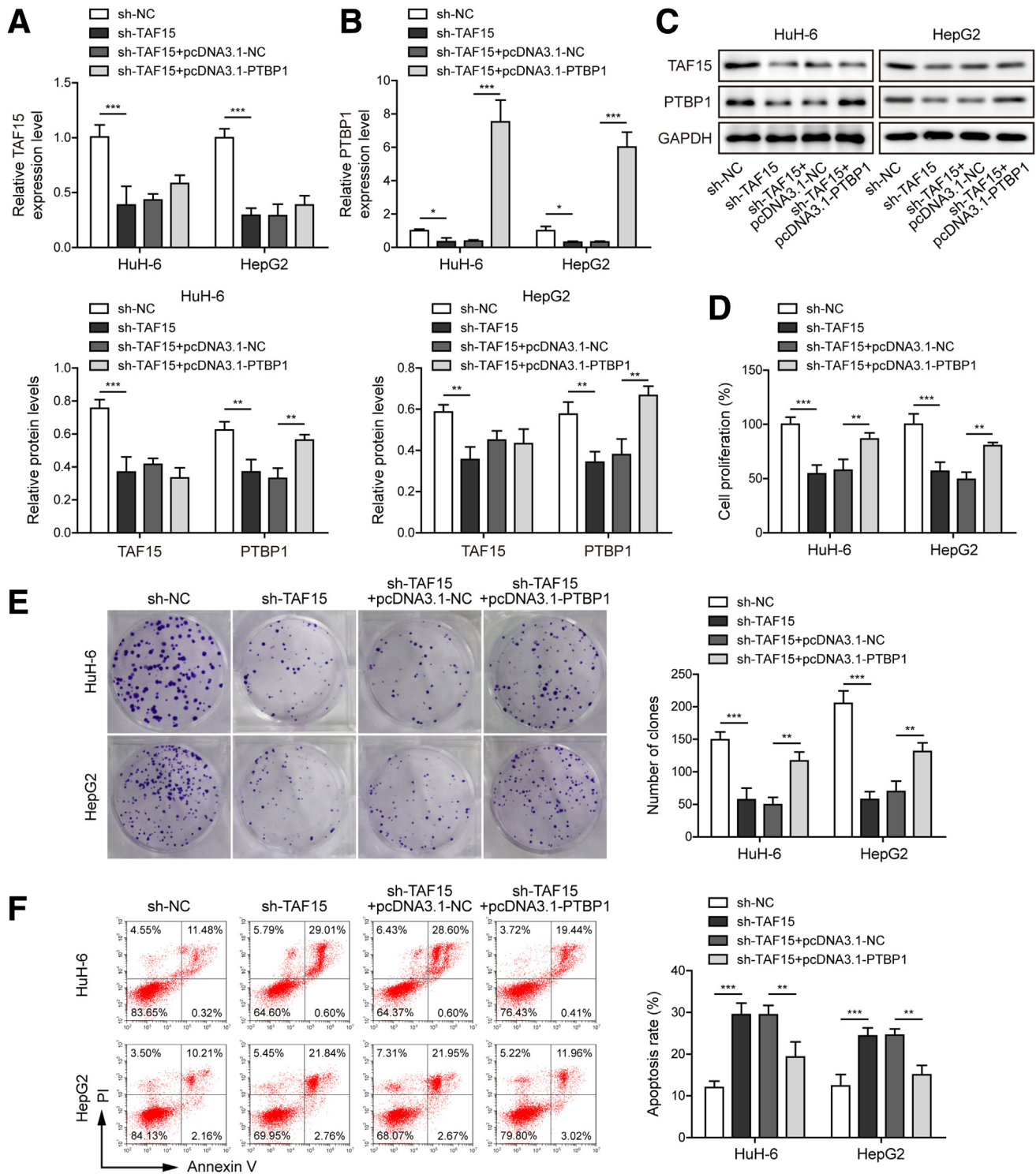
Figure 9. Overexpression of PTBP1 reversed knockdown of TAF15-mediated regulation on proliferation and apoptosis in hepatoblastoma. HuH-6 and HepG2 cells were transfected with sh-NC, sh-TAF15, sh-TAF15+pcDNA3.1-NC, or sh-TAF15+pcDNA3.1-PTBP1. Untransfected cells were used as control. (*A* and *B*) qRT-PCR analyses of TAF15 and PTBP1 in HuH-6 and HepG2 cells. (*C*) Protein levels of TAF15 and PTBP1 were assessed by Western blotting. GAPDH was used as normalization control. (*D* and *E*) Cell proliferation was evaluated by CCK-8 and colony formation assays. (*F*) Cell apoptosis was analyzed by Annexin V and PI staining. *P < .05, **P < .01, ***P < .001.

present study, we found that circ-CCT2, TAF15, and PTBP1 were up-regulated in hepatoblastoma, and circ-CCT2 activated the Wnt/β-catenin signaling and promoted the proliferation, migration, invasion, and EMT of hepatoblastoma cells via promoting TAF15 expression to stabilize PTBP1 mRNA in hepatoblastoma.
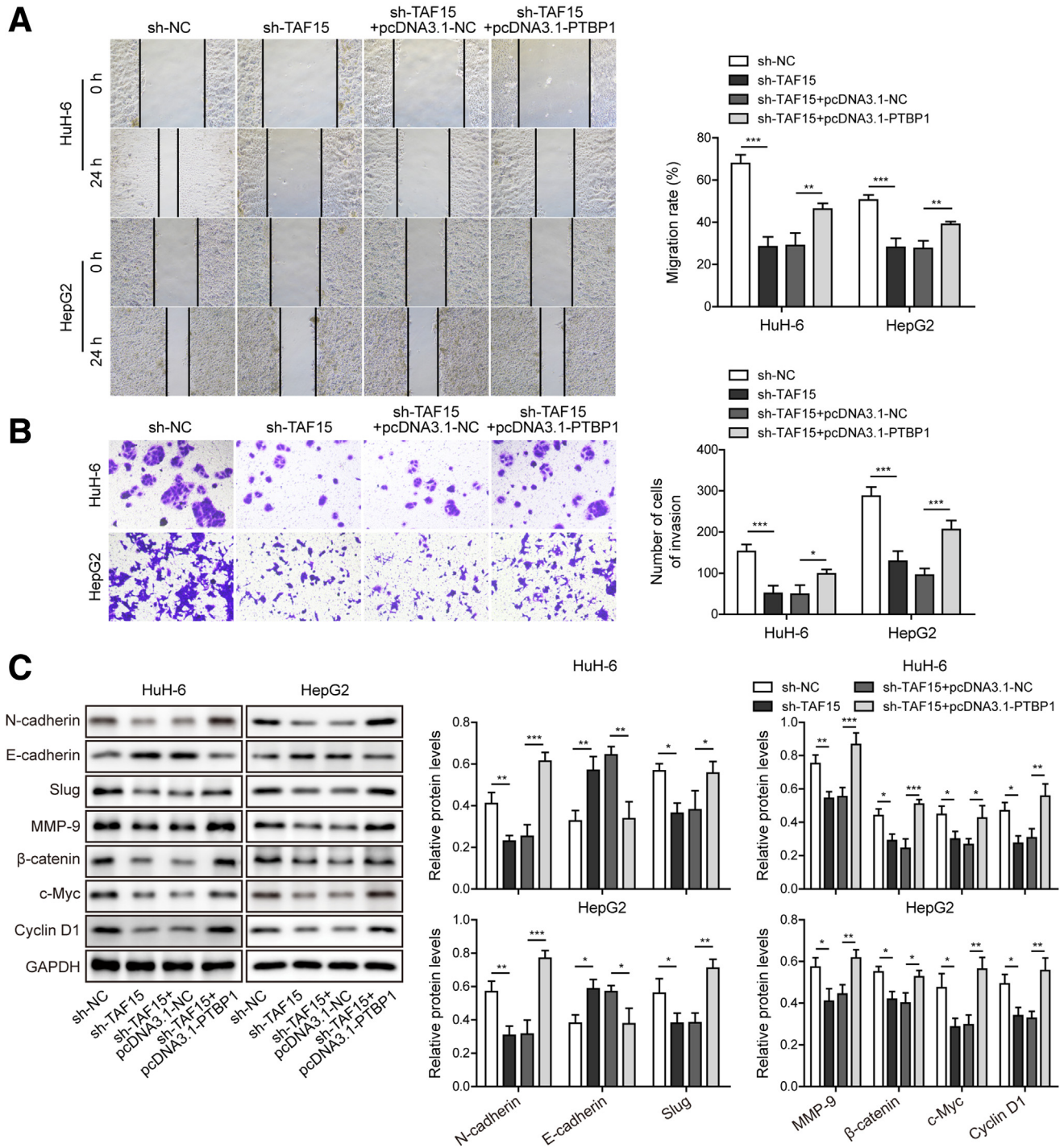
Figure 10. Overexpression of PTBP1 reversed knockdown of TAF15-mediated regulation on migration, invasion, EMT, and Wnt/β-catenin signaling in hepatoblastoma. HuH-6 and HepG2 cells were transfected with sh-NC, sh-TAF15, sh-TAF15+pcDNA3.1-NC, or sh-TAF15+pcDNA3.1-PTBP1. Untransfected cells were used as control. (*A* and *B*) Migratory and invasive capacities of HuH-6 and HepG2 cells were evaluated by wound healing and Transwell assays. (*C*) Protein levels of N-cadherin, E-cadherin, Slug, MMP-9, β-catenin, c-Myc, and Cyclin D1 in HuH-6 and HepG2 cells were analyzed by Western blotting and normalized to GAPDH. *$P < .05$, **$P < .01$, ***$P < .001$.

Although the study of circ-CCT2 in cancers is very limited, a recent study has shown that circ-CCT2 is up-regulated in glioma, and circ-CCT2 promoted growth and cell cycle progression in glioma via decoying miR-409-3p and up-regulating PDK1.[13] Here, we reported elevated expression of circ-CCT2 in hepatoblastoma for the first time. Overexpression of circ-CCT2 enhanced cell proliferation, migration, invasion, and EMT, inhibited cell apoptosis, and
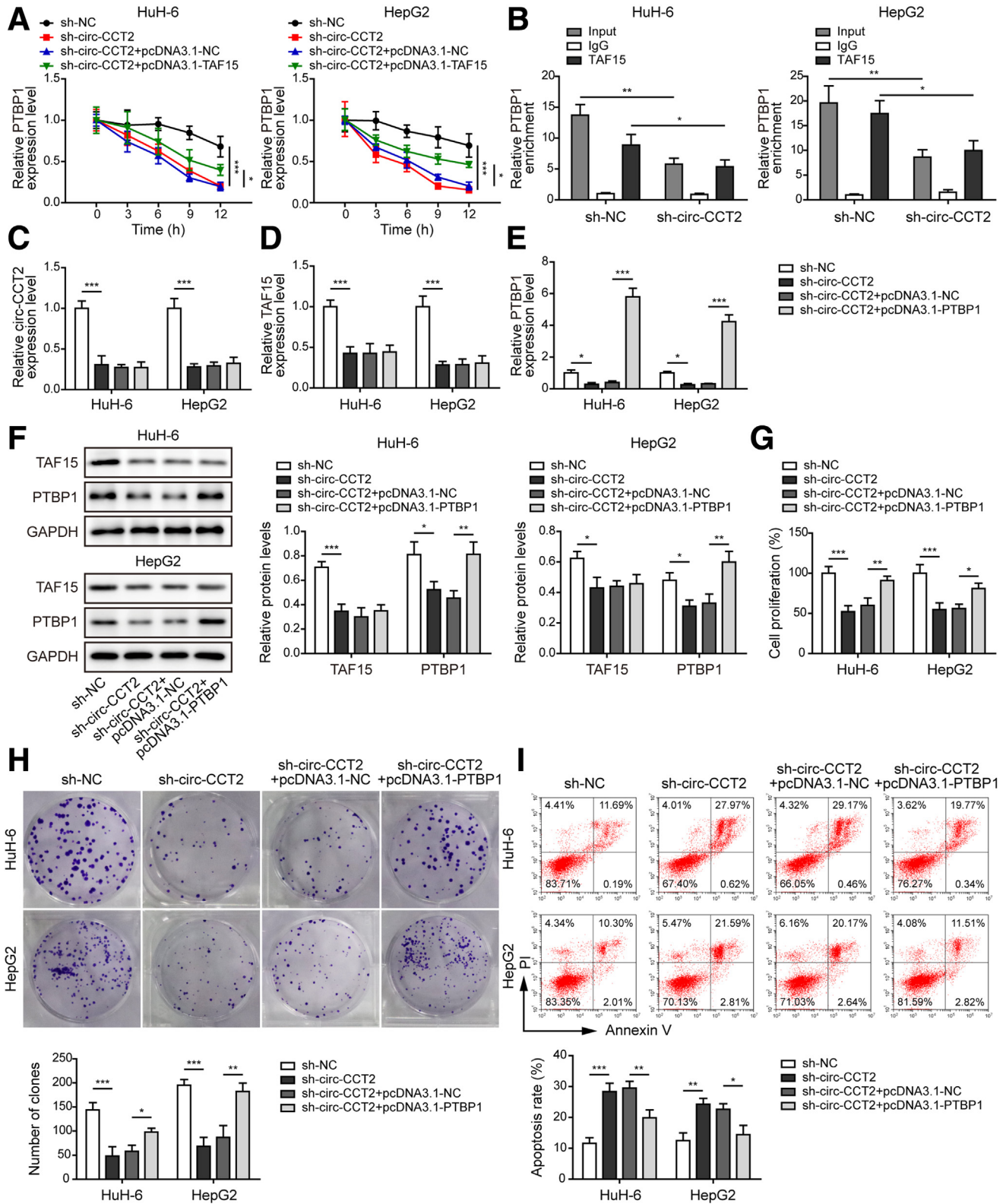
Figure 11. Overexpression of PTBP1 reversed knockdown of circ-CCT2–mediated regulation on proliferation and apoptosis in hepatoblastoma. (*A*) HuH-6 and HepG2 cells were transfected with sh-NC, sh-circ-CCT2, sh-circ-CCT2+pcDNA3.1-NC, or sh-circ-CCT2+pcDNA3.1-TAF15. Stability of PTBP1 mRNA in HuH-6 and HepG2 cells after actinomycin D treatment was examined using qRT-PCR. (*B*) HuH-6 and HepG2 cells were transfected with sh-NC or sh-circ-CCT2. Enrichment of PTBP1 mRNA was examined in input and anti-TAF15–immunoprecipitated fractions. Normal immunoglobulin G was used as negative control. HuH-6 and HepG2 cells were transfected with sh-NC, sh-circ-CCT2, sh-circ-CCT2+pcDNA3.1-NC, or sh-circ-CCT2+pcDNA3.1-PTBP1. (*C–E*) qRT-PCR analyses of circ-CCT2, TAF15, and PTBP1 expression. (*F*) Protein levels of TAF15 and PTBP1 were assessed by Western blotting. GAPDH was used as normalization control. (*G* and *H*) Cell proliferation was evaluated by CCK-8 and colony formation assays. (*I*) Cell apoptosis was analyzed by Annexin V and PI staining. $*P < .05$, $**P < .01$, $***P < .001$.
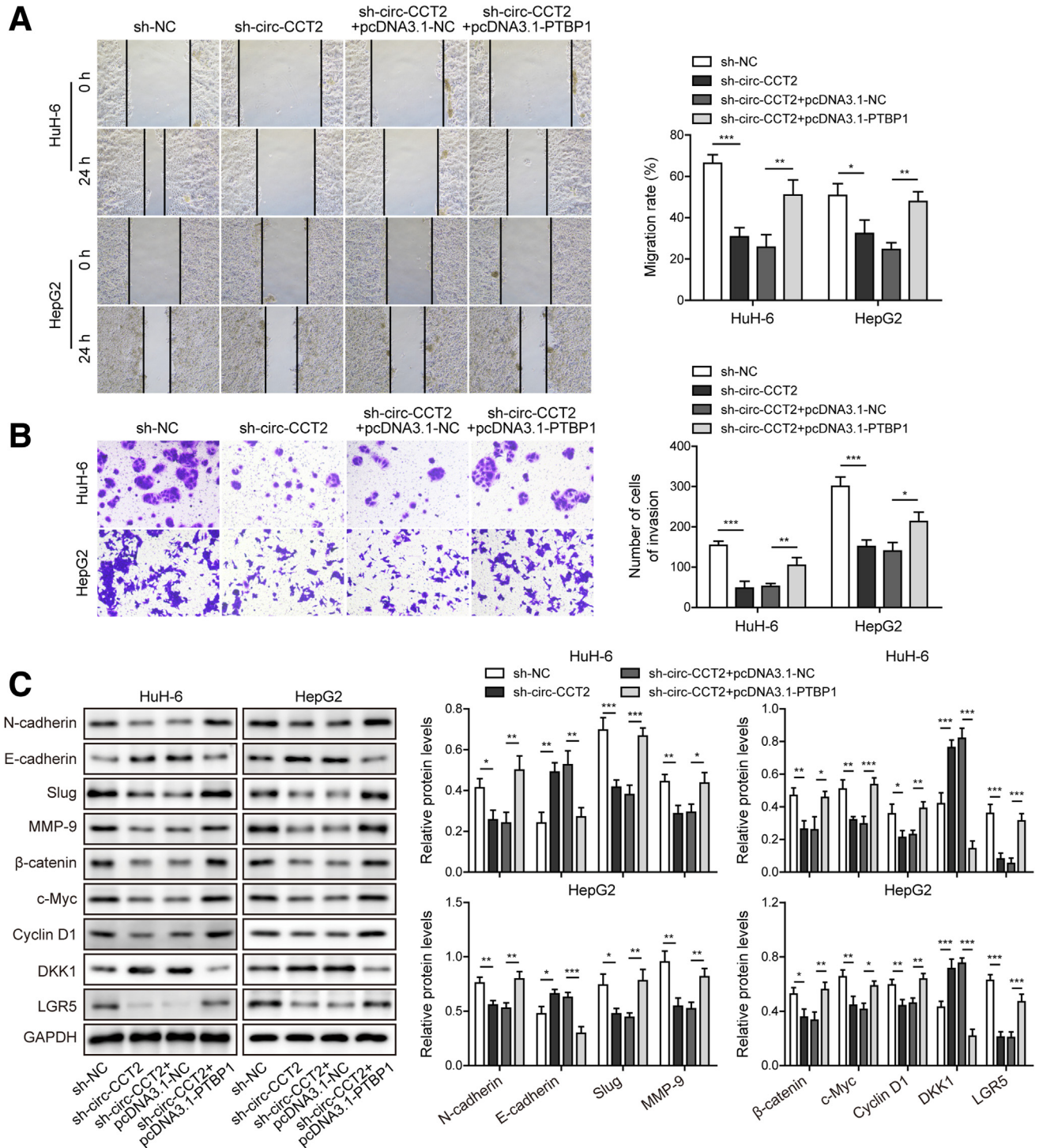
Figure 12. Overexpression of PTBP1 reversed knockdown of circ-CCT2–mediated inhibition on migration, invasion, EMT, and Wnt/β-catenin signaling in hepatoblastoma. HuH-6 and HepG2 cells were transfected with sh-NC, sh-circ-CCT2, sh-circ-CCT2+pcDNA3.1-NC, or sh-circ-CCT2+pcDNA3.1-PTBP1. (*A* and *B*) HuH-6 and HepG2 cell migration and invasion were analyzed by wound healing and Transwell assays. (*C*) Protein levels of N-cadherin, E-cadherin, Slug, MMP-9, β-catenin, c-Myc, Cyclin D1, DKK1, and LGR5 were analyzed by Western blotting. *$P < .05$, **$P < .01$, ***$P < .001$.

activated the Wnt/β-catenin signaling in hepatoblastoma, whereas knockdown of circ-CCT2 served the opposite functions. Our study first demonstrates that circ-CCT2 serves an oncogenic role in hepatoblastoma, providing a novel target for hepatoblastoma treatment. We also notice that the effects of circ-CCT2 overexpression or knockdown on subcutaneous tumor growth are greater in HepG2 than HuH-6. We suspect that the various effects of circ-CCT2
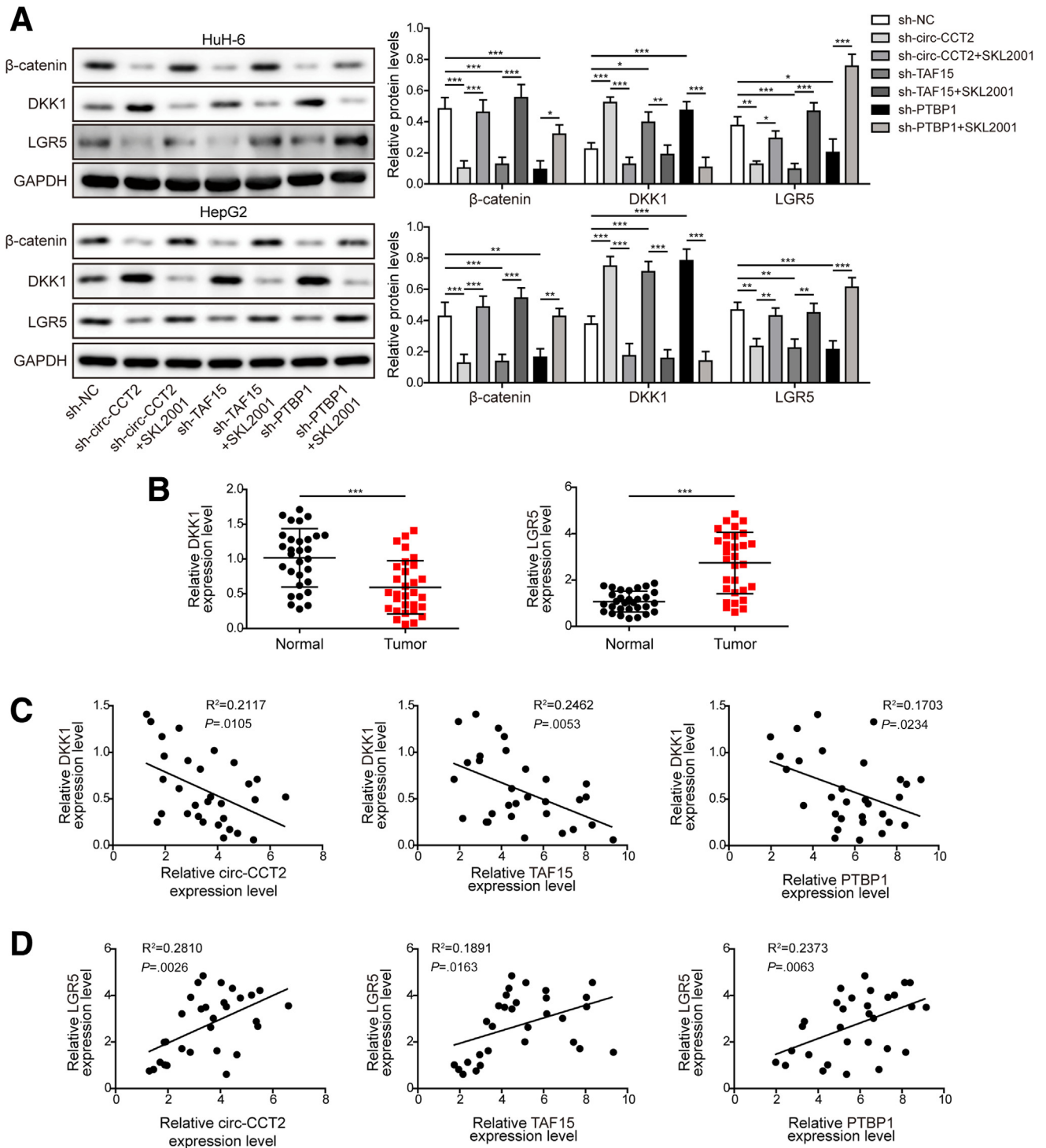
Figure 13. SKL2001 reversed knockdown of circ-CCT2, TAF15, or PTBP1–mediated inhibition of Wnt/β-catenin signaling. HuH-6 and HepG2 cells were transfected with sh-NC, sh-circ-CCT2, sh-TAF15, or sh-PTBP1 and treated with SKL2001 at 50 μmol/L for 24 hours. (*A*) Protein levels of β-catenin, DKK1, and LGR5 were analyzed by Western blotting. (*B*) qRT-PCR analysis of DKK1 and LGR5 in hepatoblastoma and adjacent normal tissues (n = 30). (*C* and *D*) Correlation analysis of DKK1 or LGR5 expression with expression of circ-CCT2, TAF15, and PTBP1 in hepatoblastoma tissues (n = 30). *$P < .05$, **$P < .01$, ***$P < .001$.

overexpression or knockdown on subcutaneous tumor growth in different cells may result from complex reasons such as different in vivo tumorigenicity of HepG2 and HuH-6 cells, various transfection efficiency of circ-CCT2 overexpression or knockdown in HepG2 and HuH-6 cells, or different resistance degree of mice against HepG2 and HuH-6 cells.
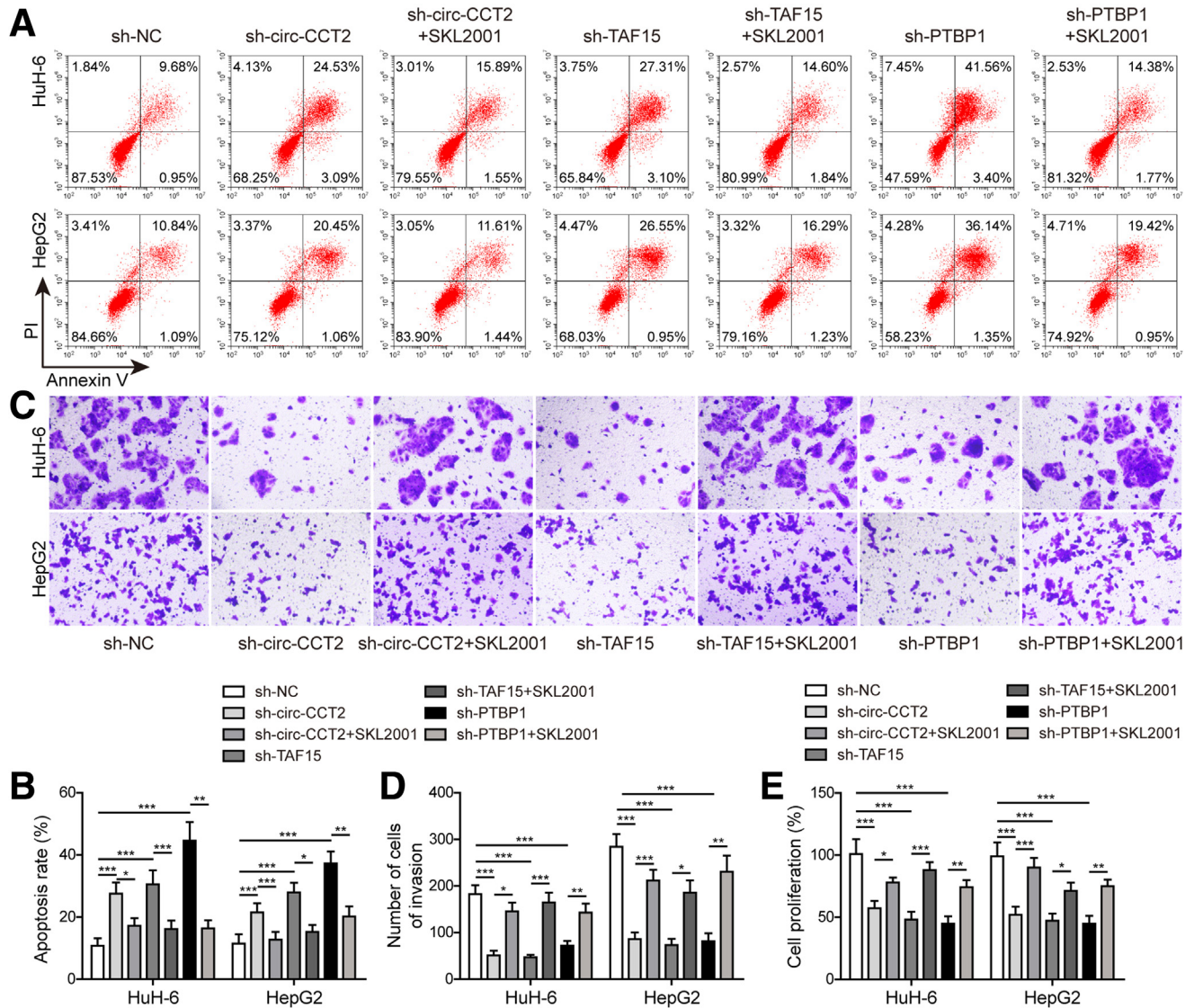
Figure 14. Activation of Wnt/β-catenin signaling reversed knockdown of circ-CCT2, TAF15, or PTBP1–mediated inhibition of malignant phenotypes of hepatoblastoma. HuH-6 and HepG2 cells were transfected with sh-NC, sh-circ-CCT2, sh-TAF15, or sh-PTBP1 and treated with SKL2001 at 50 μmol/L for 24 hours. (*A* and *B*) HuH-6 and HepG2 cell apoptosis was analyzed by Annexin V and PI staining. (*C* and *D*) HuH-6 and HepG2 cell invasion was analyzed by Transwell assay. (*E*) Cell proliferation was evaluated by CCK-8 assay. *$P < .05$, **$P < .01$, ***$P < .001$.

It has been well-acknowledged that circRNAs function as miRNA sponges to regulate tumor progression,[35,36] and circRNAs also interact with proteins to exert biological functions.[19,37] CircMYBL2 was reported to recruit PTBP1 to modulate FLT3 translation and promote the progression of FLT3-ITD acute myeloid leukemia.[38] CircMRPS35 inhibited the progression of gastric cancer by recruiting KAT7 to control histone modification.[39] Here, we first observed elevated TAF15 expression in hepatoblastoma and confirmed the interaction between circ-CCT2 and TAF15 by RIP and RNA pull-down assays. Moreover, circ-CCT2 and TAF15 co-localized in the cytoplasm of hepatoblastoma cells and tissues as shown by FISH combined IF assays. Furthermore, overexpression of TAF15 reversed knockdown of circ-CCT2–mediated inhibition of hepatoblastoma

progression. Our study is the first evidence to indicate that circ-CCT2 promotes hepatoblastoma progression via recruiting TAF15 to the cytoplasm and also up-regulating TAF15 expression.

As an RNA binding protein, TAF15 can stabilize target mRNAs via binding to G-rich sequences.[40] TAF15 has been reported to maintain the stability of HMGB3 and TRPM2 mRNAs and lncRNA LINC00665.[18,41,42] Therefore, we predicted that PTBP1 was a potential mRNA target of TAF15 by bioinformatics. TAF15 expression was positively correlated with PTBP1 expression in hepatoblastoma, and the direct interaction between TAF15 protein and PTBP1 mRNA was validated. We identified a novel mRNA target of TAF15 and demonstrated that TAF15 stabilized PTBP1 mRNA in hepatoblastoma. Besides, knockdown of TAF15 or circ-

CCT2–mediated suppression of hepatoblastoma progression was reversed by PTBP1. Circ-CCT2 might regulate PTBP1 expression via 2 potential mechanisms: (1) circ-CCT2 increases TAF15 expression to promote the stability of PTBP1 mRNA and its expression; and (2) circ-CCT2 facilitates the enrichment of PTBP1 mRNA to TAF15 protein. In our study, we confirmed the first mechanism occurred in hepatoblastoma. However, we could not ensure equal amount of TAF15 protein was pulled down to allow fair comparison of the bound PTBP1 mRNA between the circ-CCT2 knockdown cells and the control cells. Thus, we do not have enough evidence demonstrating the second possibility that circ-CCT2 regulates PTBP1 expression via modulating the binding of TAF15 to PTBP1 mRNA, and it needs further investigation. We therefore first proved that circ-CCT2 promoted TAF15 expression to maintain the stability of PTBP1 mRNA, thus regulating hepatoblastoma progression.

PTBP1 is a vital modulator in the activation of Wnt/β-catenin signaling,[25,43] which is highly activated in human cancers.[44,45] Consistently, the activated Wnt/β-catenin signaling was observed in hepatoblastoma. Knockdown of circ-CCT2 or TAF15 could suppress Wnt/β-catenin signaling as shown by the down-regulation of β-catenin, c-Myc, Cyclin D1, and LGR5 and up-regulation of DKK1, but overexpression of PTBP1 reversed these effects. Activation of Wnt/β-catenin signaling through SKL2001 treatment abrogated the anti-tumor activities of circ-CCT2, TAF15, or PTBP1 knockdown. Our study supports the notion that circ-CCT2 regulates hepatoblastoma progression through the activation of Wnt/β-catenin signaling.

Conclusion

We first demonstrated that circ-CCT2 promoted hepatoblastoma progression and activated Wnt/β-catenin signaling by recruiting and up-regulating TAF15 protein to stabilize PTBP1 mRNA. Our findings identify a novel and significant contribution of circ-CCT2 to the progression of hepatoblastoma. Targeting circ-CCT2 may be potentially used for hepatoblastoma intervention. However, more samples from hepatoblastoma patients and animal models of hepatoblastoma should be involved in further investigations for clinical application. Also, our study lacks big data analysis because of disease limitation. Another limitation is that we do not know the regulatory mechanism by which circ-CCT2 is up-regulated in hepatoblastoma. Studies are ongoing to overcome these limitations to clarify the nature of the regulation of hepatoblastoma progression in detail.

Materials and Methods
Clinical Specimens

Hepatoblastoma and adjacent normal tissues were obtained from hepatoblastoma patients at Xiangya Hospital, Central South University and stored at –80°C for subsequent RNA extraction and analysis of the expression of circ-CCT2, TAF15, PTBP1, dickkopf-1 (DKK1), and leucine-rich repeat-containing G protein-coupled receptor 5 (LGR5). Written informed consent was provided by patients. Our study got approval from the Ethics Committee of Xiangya Hospital, Central South University. The clinicopathologic characteristics of patients enrolled in the study were included in Table 1.

Cell Culture and Transfection

Normal human hepatic cell line L-02 and MIHA and hepatoblastoma cell lines HuH-6 and HepG2 provided by the Cell Bank of Chinese Academy of Sciences (Shanghai, China) were cultured in Dulbecco modified Eagle medium containing 10% fetal bovine serum (Gibco, Grand Island, NY) and 1% penicillin and streptomycin (Gibco) in a humidified incubator at 37°C with 5% CO_2. To activate Wnt/β-catenin signaling, cells were treated with SKL2001 (Selleck, Houston, TX) at 50 μmol/L for 24 hours.

The coding sequences of TAF15 and PTBP1 were cloned into the pcDNA3.1 vector (pcDNA3.1-TAF15 and pcDNA3.1-PTBP1; Thermo Fisher Scientific, Waltham, MA). The empty pcDNA3.1 vector was used as a negative control (pcDNA3.1-NC). ShRNAs against circ-CCT2 (sh-circ-CCT2), TAF15 (sh-TAF15), and PTBP1 (sh-PTBP1) and scramble controls (sh-NC) were synthesized by RiboBio (Guangzhou, China). For lentiviral transduction, circ-CCT2 was inserted into the pCDH lentiviral vector (Addgene, Watertown, MA), and sh-circ-CCT2 was cloned into the pLKO.1 lentiviral vector (Addgene). The empty pCDH vector (OE-NC) and pLKO.1 containing scramble sequence (sh-NC) were used as negative controls. Lentiviral particles were packaged in HEK293T cells, and HuH-6 and HepG2 cells were infected with lentiviral particles for stable overexpression or knockdown of circ-CCT2. For transient transfection, HuH-6 and HepG2 cells were transfected with pcDNA3.1-NC, pcDNA3.1-TAF15, pcDNA3.1-PTBP1, sh-NC, sh-PTBP1, or sh-TAF15 with Lipo3000 transfection reagent (Thermo Fisher Scientific).

FISH and IF Staining

For FISH assay, HuH-6 and HepG2 cells were seeded on coverslips and fixed in methanol/acetic acid solution. Subsequently, coverslips were air-dried and pre-dehydrated in ethanol. The Alexa Fluor 594-conjugated circ-CCT2 probe was denatured for 10 minutes at 80°C. Coverslips were incubated at 72°C for 5 minutes for denaturation and immersed in ethanol for re-dehydration. Subsequently, coverslips were immersed in hybridization solution and probed with the Alexa Fluor 594-conjugated circ-CCT2 probe (RiboBio) at 30 nmol/L at 37°C for 16 hours. Next day, coverslips were washed, stained with DAPI (Beyotime), and mounted for imaging under a Leica confocal microscope (Wetzlar, Germany).

Combined FISH and IF staining was applied to detect the colocalization of TAF15 protein and circ-CCT2 or PTBP1 mRNA in tissues and cells as described with some modification.[46] Briefly, clinical tissue sections or hepatoblastoma cell lines HuH-6 and HepG2 were seeded on coverslips and fixed in 4% paraformaldehyde solution for 20 minutes. Then, samples were permeabilized in 0.3% Triton X-100 and 1% bovine serum albumin solution for 1 hour. Cells and

Table 1. Correlation Between Circ-CCT2 and Clinicopathologic Features of Hepatoblastoma Patients

Features	circ-CCT2 expression		P value
	Low	High	
Age (y)			.4497
≥24	8	11	
< 24	7	4	
Sex			.2723
Male	6	10	
Female	9	5	
Stages			.0656
I-II	11	5	
III-IV	4	10	
Tumor size (cm^3)			.2320
≥500	9	12	
< 500	6	3	
Metastasis			.0281
Yes	4	10	
No	11	5	

sections were incubated with a rabbit anti-TAF15 (1:200; Abcam, Cambridge, UK) antibody at 4°C overnight. Next day, samples were washed and incubated with an Alexa Fluor 488-conjugated goat anti-rabbit immunoglobulin G (1:2000; Thermo Fisher Scientific) antibody for 1 hour. Then, samples were washed, re-fixed in 4% paraformaldehyde solution for 10 minutes, and equilibrated. Subsequently, samples were incubated in hybridization buffer containing the circ-CCT2 or PTBP1 probe (50 nmol/L) at 37°C overnight. Last, samples were washed, stained with DAPI (Beyotime), and mounted for imaging under a Leica confocal microscope.

Sanger Sequencing

Circ-CCT2 was amplified and cloned into a T-vector (Takara). Sanger sequencing (Sangon Biotech) was performed to validate the head-to-tail spliced structure of circ-CCT2.

RIP Assay

HuH-6 and HepG2 cells were lysed, and cell lysates were collected. Magnetic beads were pre-coated with a TAF15 antibody (Abcam) and mixed well with cell lysates. A normal immunoglobulin G was used as a negative control. Cell lysates were incubated with magnetic beads at 4°C overnight with gentle rotation. Next day, magnetic beads were washed and collected with a magnet. Subsequently, RNA was recovered from immunoprecipitated fractions, and the expression of circ-CCT2 and PTBP1 was analyzed with qRT-PCR.

RNA Pull-Down Assay

HuH-6 and HepG2 cells were lysed, and cell lysates were collected. The biotin-conjugated sense or anti-sense circ-CCT2 probe was mixed well with cell lysates and incubated at 4°C for 4 hours. Then, streptavidin-conjugated magnetic beads were added into samples and incubated for additional 2 hours at 4°C with gentle rotation. Subsequently, fractions pulled down by circ-CCT2 probes were eluted, and the abundance of TAF15 was examined by Western blotting.

Stability Detection of Circ-CCT2 and PTBP1 mRNA

Total RNA extracted from HuH-6 and HepG2 cells was quantified, and 5 μg of RNA was digested with RNase R (5 U/μg; Sigma-Aldrich, St Louis, MO). RNA was recovered, and the abundance of circ-CCT2 and CCT2 mRNA was analyzed by qRT-PCR. Cells were treated with actinomycin D (5 μg/mL; Sigma-Aldrich) for 0, 4, 8, 12, and 24 hours (circ-CCT2 and CCT2 mRNA) or 0, 3, 6, 9, and 12 hours (PTBP1 mRNA). Subsequently, RNA was extracted, and the abundance of circ-CCT2, CCT2, and PTBP1 mRNA was examined by qRT-PCR.

Cell Counting Kit-8 Assay

Cells were seeded in 96-well plates, and culture medium was replaced with 100 μL of fresh medium. Ten μL of CCK-8 reagent (Sigma-Aldrich) was added into medium. Cells were incubated for additional 4 hours, and the absorbance (450 nm) was measured with the Multiskan SkyHigh microplate reader (Thermo Fisher Scientific).

Colony Formation Assay

HuH-6 and HepG2 cells were transfected as indicated, and 1×10^3 cells were seeded in each well of 6-well plates. Cells were cultured for 2 weeks, and cell colonies were fixed and stained with crystal violet (0.1%; Selleck) for 30 minutes. After wash, cell colonies were imaged using the BX51 microscope (Olympus, Tokyo, Japan).

Cell Apoptosis Analysis

The Annexin V-FITC/PI apoptosis kit (Solarbio, Beijing, China) was used to analyze cell apoptosis following the manual. Briefly, HuH-6 and HepG2 cells transfected as indicated were suspended in Annexin V binding buffer and stained with 5 μL of Annexin V-FITC and 5 μL of propidium iodide (PI) for 20 minutes in dark. Cell apoptosis was analyzed immediately using a flow cytometer (Beckman Coulter, San Jose, CA).

Transwell Assay

Transwell chambers with 8-μm pore membrane were purchased from Corning (Corning, NY). For cell invasion analysis, the upper chamber was pre-coated with Matrigel (BD, Franklin Lakes, NJ). HuH-6 and HepG2 cells (1×10^5 cells) with indicated transfection were seeded into the upper chamber and cultured for 24 hours. Cells that invaded into the lower chambers were washed, fixed, and stained with 0.1% crystal violet (Selleck) for 30 minutes. Cells were imaged using the BX51 microscope (Olympus).

Wound Healing Assay

HuH-6 and HepG2 cells with indicated transfection were seeded and grown to form a confluent monolayer. The cell monolayer was scraped with cell combs from EMD Millipore (Darmstadt, Germany) and cultured for 24 hours for wound healing. Wound healing was observed under a BX51 microscope (Olympus) and quantified with the Image J software.

Subcutaneous Mouse Model of Hepatoblastoma

Fifty-six male BALB/c nude mice (6-week-old; SLAC Laboratory Animal Center, Shanghai, China) were divided into 8 groups (n = 7 in each group). HuH-6 and HepG2 cells were stably transfected with OE-NC, OE-circ-CCT2, sh-NC, or sh-circ-CCT2 through lentiviral transduction and subcutaneously injected into the left flanks of mice (2×10^6 cells to each mouse). Tumor size was measured at days 7, 14, 21, and 28, and tumor volume was calculated with the formula length $\times$ width^2/2. Finally, mice were killed. Tumors were excised and weighed. Animal experiments were approved by the Animal Care and Use Committee of Xiangya Hospital, Central South University.

Immunohistochemistry Staining

Subcutaneous tumors were embedded in paraffin and sliced into 5-μm sections. Sections were deparaffinized, rehydrated, and retrieved in antigen retrieval buffer (Abcam). Subsequently, sections were incubated in H_2O_2 solution for 10 minutes, blocked, and incubated with a rabbit Ki-67 (1:50; Abcam) or N-cadherin (1:100; Abcam) antibody for 2 hours. After washing, sections were incubated with horseradish peroxidase–conjugated goat anti-rabbit antibody for 1 hour. Signals were visualized with DAB from Abcam. Sections were stained with hematoxylin and imaged under a BX51 microscope (Olympus).

qRT-PCR

Hepatoblastoma and adjacent normal tissues were homogenized, and total RNA was extracted from tissue homogenates and hepatoblastoma cells using Trizol (Beyotime) before quantification with NanoDrop. Subsequently, RNA was reversely transcribed into cDNA with PrimeScript RT reagent kit (Takara, Dalian, China). Circ-CCT2, CCT2, TAF15, PTBP1, DKK1, and LGR5 were examined by real-time qPCR with SYBR Green Master Mix (Thermo Fisher Scientific) and normalized to GAPDH. The $2^{-\Delta\Delta Ct}$ method was applied for calculation. Primers were ordered from Sangon Biotech (Shanghai, China).

Western blotting

Tumors were excised and homogenized in cold lysis buffer. The supernatants were collected from tissue homogenates and cell lysates for protein quantification. Protein (30 μg) was electrophoresed and transferred to polyvinylidene difluoride membranes (Bio-Rad, Hercules, CA). Subsequently, membranes were blocked and incubated with rabbit TAF15 (1:2000), PTBP1 (1:1000; Thermo Fisher Scientific), E-cadherin (1:1000), N-cadherin (1:1000), Slug (1:2000; Thermo Fisher Scientific), MMP-9 (1:1000), β-catenin (1:1000), c-Myc (1:5000), Cyclin D1 (1:1000), DKK1 (1:1000), LGR5 (1:1500), and GAPDH (1:5000; Thermo Fisher Scientific) antibodies. Primary antibodies were provided by Abcam unless otherwise indicated. Membranes were washed and incubated with horseradish peroxidase–conjugated goat anti-rabbit immunoglobulin G antibody. The ECL substrate (Bio-Rad) was added to visualize the bands, and band intensity was analyzed with the Image J software.

Statistical Analysis

Data in present study were from at least 3 independent experiments and shown as mean ± standard deviation. Data were analyzed with Prism 6.0 (GraphPad Software, San Diego, CA). The Student t test or one-way analysis of variance was used for comparing the variance between 2 or multiple groups, respectively. $P < .05$ was statistically significant.

References

1. Chattopadhyay S, Mukherjee S, Boler A, et al. Hepatoblastoma in the neonatal period: an unusual presentation. Journal of Cytology 2012;29:252–254.
2. Finegold MJ, Egler RA, Goss JA, et al. Liver tumors: pediatric population. Liver Transpl 2008;14:1545–1556.
3. Allan BJ, Parikh PP, Diaz S, et al. Predictors of survival and incidence of hepatoblastoma in the paediatric population. HPB 2013;15:741–746.
4. Hubbard AK, Spector LG, Fortuna G, et al. Trends in international incidence of pediatric cancers in children under 5 years of age: 1988-2012. JNCI Cancer Spectrum 2019;3:pkz007.
5. Ismail H, Broniszczak D, Kalicinski P, et al. Changing treatment and outcome of children with hepatoblastoma: analysis of a single center experience over the last 20 years. J Pediatr Surg 2012;47:1331–1339.
6. Roebuck DJ, Perilongo G. Hepatoblastoma: an oncological review. Pediatr Radiol 2006;36:183–186.
7. Zhong Y, Du Y, Yang X, et al. Circular RNAs function as ceRNAs to regulate and control human cancer progression. Molecular Cancer 2018;17:79.
8. Zhen N, Gu S, Ma J, et al. CircHMGCS1 promotes hepatoblastoma cell proliferation by regulating the IGF signaling pathway and glutaminolysis. Theranostics 2019;9:900–919.
9. Chen L, Shi J, Wu Y, et al. CircRNA CDR1as promotes hepatoblastoma proliferation and stemness by acting as a miR-7-5p sponge to upregulate KLF4 expression. Aging 2020;12:19233–19253.
10. Liu Y, Song J, Liu Y, et al. Transcription activation of circ-STAT3 induced by Gli2 promotes the progression of hepatoblastoma via acting as a sponge for miR-29a/b/c-3p to upregulate STAT3/Gli2. J Exp Clin Cancer Res 2020;39:101.
11. Carr AC, Khaled AS, Bassiouni R, et al. Targeting chaperonin containing TCP1 (CCT) as a molecular

therapeutic for small cell lung cancer. Oncotarget 2017; 8:110273–110288.

12. Showalter AE, Martini AC, Nierenberg D, et al. Investigating chaperonin-containing TCP-1 subunit 2 as an essential component of the chaperonin complex for tumorigenesis. Scientific Reports 2020;10:798.

13. Ma Z, Chen Z, Zhou Y, et al. Hsa_circ_0000418 promotes the progression of glioma by regulating microRNA-409-3p / pyruvate dehydrogenase kinase 1 axis. Bioengineered 2022;13:7541–7552.

14. Law WJ, Cann KL, Hicks GG. TLS, EWS and TAF15: a model for transcriptional integration of gene expression. Briefings in Functional Genomics & Proteomics 2006; 5:8–14.

15. Bertolotti A, Lutz Y, Heard DJ, et al. hTAF(II)68, a novel RNA/ssDNA-binding protein with homology to the pro-oncoproteins TLS/FUS and EWS is associated with both TFIID and RNA polymerase II. EMBO J 1996; 15:5022–5031.

16. Kapeli K, Martinez FJ, Yeo GW. Genetic mutations in RNA-binding proteins and their roles in ALS. Hum Genet 2017;136:1193–1214.

17. Kapeli K, Pratt GA, Vu AQ, et al. Distinct and shared functions of ALS-associated proteins TDP-43, FUS and TAF15 revealed by multisystem analyses. Nature Communications 2016;7:12143.

18. Ren P, Xing L, Hong X, et al. LncRNA PITPNA-AS1 boosts the proliferation and migration of lung squamous cell carcinoma cells by recruiting TAF15 to stabilize HMGB3 mRNA. Cancer Medicine 2020; 9:7706–7716.

19. Huang A, Zheng H, Wu Z, et al. Circular RNA-protein interactions: functions, mechanisms, and identification. Theranostics 2020;10:3503–3517.

20. Wang X, Li Y, Fan Y, et al. PTBP1 promotes the growth of breast cancer cells through the PTEN/Akt pathway and autophagy. J Cell Physiol 2018;233:8930–8939.

21. Xiao M, Liu J, Xiang L, et al. MAFG-AS1 promotes tumor progression via regulation of the HuR/PTBP1 axis in bladder urothelial carcinoma. Clinical and Translational Medicine 2020;10:e241.

22. Kang H, Heo S, Shin JJ, et al. A miR-194/PTBP1/CCND3 axis regulates tumor growth in human hepatocellular carcinoma. J Pathol 2019;249:395–408.

23. Taniguchi K, Uchiyama K, Akao Y. PTBP1-targeting microRNAs regulate cancer-specific energy metabolism through the modulation of PKM1/M2 splicing. Cancer Science 2021;112:41–50.

24. Jiang W, Ou ZL, Zhu Q, et al. LncRNA OIP5-AS1 aggravates the stemness of hepatoblastoma through recruiting PTBP1 to increase the stability of beta-catenin. Pathol Res Pract 2022;232:153829.

25. He X, Sheng J, Yu W, et al. LncRNA MIR155HG promotes temozolomide resistance by activating the Wnt/beta-catenin pathway via binding to PTBP1 in glioma. Cellular and Molecular Neurobiology 2021;41:1271–1284.

26. Sheng J, He X, Yu W, et al. p53-targeted lncRNA ST7-AS1 acts as a tumour suppressor by interacting with PTBP1 to suppress the Wnt/beta-catenin signalling pathway in glioma. Cancer Letters 2021;503:54–68.

27. Meng S, Zhou H, Feng Z, et al. CircRNA: functions and properties of a novel potential biomarker for cancer. Molecular Cancer 2017;16:94.

28. Rybak-Wolf A, Stottmeister C, Glazar P, et al. Circular RNAs in the mammalian brain are highly abundant, conserved, and dynamically expressed. Molecular Cell 2015;58:870–885.

29. Xu X, Zhang J, Tian Y, et al. CircRNA inhibits DNA damage repair by interacting with host gene. Molecular Cancer 2020;19:128.

30. Jeck WR, Sorrentino JA, Wang K, et al. Circular RNAs are abundant, conserved, and associated with ALU repeats. RNA 2013;19:141–157.

31. Du WW, Zhang C, Yang W, et al. Identifying and characterizing circRNA-protein interaction. Theranostics 2017;7:4183–4191.

32. Feng J, Polychronidis G, Heger U, et al. Incidence trends and survival prediction of hepatoblastoma in children: a population-based study. Cancer Communications 2019; 39:62.

33. Wang YX, Liu H. Adult hepatoblastoma: systemic review of the English literature. Dig Surg 2012;29:323–330.

34. Zheng MH, Zhang L, Gu DN, et al. Hepatoblastoma in adult: review of the literature. Journal of Clinical Medicine Research 2009;1:13–16.

35. Zhang X, Wang S, Wang H, et al. Circular RNA circNRIP1 acts as a microRNA-149-5p sponge to promote gastric cancer progression via the AKT1/mTOR pathway. Molecular Cancer 2019;18:20.

36. Han D, Li J, Wang H, et al. Circular RNA circMTO1 acts as the sponge of microRNA-9 to suppress hepatocellular carcinoma progression. Hepatology 2017;66:1151–1164.

37. Zhou WY, Cai ZR, Liu J, et al. Circular RNA: metabolism, functions and interactions with proteins. Molecular Cancer 2020;19:172.

38. Sun YM, Wang WT, Zeng ZC, et al. circMYBL2, a circRNA from MYBL2, regulates FLT3 translation by recruiting PTBP1 to promote FLT3-ITD AML progression. Blood 2019;134:1533–1546.

39. Jie M, Wu Y, Gao M, et al. CircMRPS35 suppresses gastric cancer progression via recruiting KAT7 to govern histone modification. Molecular Cancer 2020;19:56.

40. Dominguez D, Freese P, Alexis MS, et al. Sequence, structure, and context preferences of human RNA binding proteins. Molecular Cell 2018;70:854–867 e859.

41. Pan L, Li Y, Jin L, et al. TRPM2-AS promotes cancer cell proliferation through control of TAF15. Int J Biochem Cell Biol 2020;120:105683.

42. Ruan X, Zheng J, Liu X, et al. lncRNA LINC00665 stabilized by TAF15 impeded the malignant biological behaviors of glioma cells via STAU1-mediated mRNA degradation. Molecular Therapy Nucleic Acids 2020;20:823–840.

43. Yao XY, Liu JF, Luo Y, et al. LncRNA HOTTIP facilitates cell proliferation, invasion, and migration in osteosarcoma by interaction with PTBP1 to promote KHSRP level. Cell Cycle 2021;20:283–297.

44. Zhan T, Rindtorff N, Boutros M. Wnt signaling in cancer. Oncogene 2017;36:1461–1473.

45. Polakis P. Wnt signaling in cancer. Cold Spring Harbor Perspectives in Biology 2012;4.

46. Kochan J, Wawro M, Kasza A. Simultaneous detection of mRNA and protein in single cells using immunofluorescence-combined single-molecule RNA FISH. BioTechniques 2015;59:209–212, 214, 216 passim.

Correspondence
Address correspondence to: Hong-Yan Zai, MD, Department of General Surgery, Xiangya Hospital, Central South University, No. 87 Xiangya Road, Changsha 41008, Hunan Province, P.R. China. e-mail: zaihy@csu.edu.cn.

CRediT Authorship Contributions
Qin Zhu (Conceptualization: Lead; Data curation: Lead)
Yu Hu (Formal analysis: Lead; Funding acquisition: Lead)
Wei Jiang (Investigation: Lead; Methodology: Lead)
Zheng-Lin Ou (Software: Lead; Supervision: Lead)
Yuan-Bing Yao (Project administration: Lead; Visualization: Lead; Writing – original draft: Lead; Writing – review & editing: Lead)
Hong-Yan Zai (Writing – original draft: Equal; Writing – review & editing: Equal)

Conflicts of interest
The authors disclose no conflicts.